

Discovery of Aminothiazole Inhibitors of Cyclin-Dependent Kinase 2: Synthesis, X-ray Crystallographic Analysis, and Biological Activities

Kyoung Soon Kim,^{*,†} S. David Kimball,[‡] Raj N. Misra,[†] David B. Rawlins,[†] John T. Hunt,[§] Hai-Yun Xiao,[†] Songfeng Lu,[†] Ligang Qian,[†] Wen-Ching Han,[†] Weifang Shan,[†] Toomas Mitt,[†] Zhen-Wei Cai,^{||} Michael A. Poss,^{||} Hong Zhu,^{||} John S. Sack,[⊥] John S. Tokarski,[⊥] Chieh Ying Chang,[⊥] Nikola Pavletich,[#] Amrita Kamath,[∇] William G. Humphreys,[∇] Punit Marathe,[∇] Isia Bursuker,[○] Kristen A. Kellar,[§] Urvashi Roongta,[§] Roberta Batorsky,[§] Janet G. Mulheron,[§] David Bol,[§] Craig R. Fairchild,[§] Francis Y. Lee,[§] and Kevin R. Webster[^]

Departments of Oncology Chemistry, Oncology Drug Discovery, New Leads Chemistry, Structural Biology and Modeling, Metabolism and Pharmacokinetics, and High Throughput Screening, Bristol-Myers Squibb Pharmaceutical Research Institute, Princeton, New Jersey 08543-4000

Received April 9, 2002

High throughput screening identified 2-acetamido-thiazolylthio acetic ester **1** as an inhibitor of cyclin-dependent kinase 2 (CDK2). Because this compound is inactive in cells and unstable in plasma, we have stabilized it to metabolic hydrolysis by replacing the ester moiety with a 5-ethyl-substituted oxazole as in compound **14**. Combinatorial and parallel synthesis provided a rapid analysis of the structure–activity relationship (SAR) for these inhibitors of CDK2, and over 100 analogues with IC₅₀ values in the 1–10 nM range were rapidly prepared. The X-ray crystallographic data of the inhibitors bound to the active site of CDK2 protein provided insight into the binding modes of these inhibitors, and the SAR of this series of analogues was rationalized. Many of these analogues displayed potent and broad spectrum antiproliferative activity across a panel of tumor cell lines in vitro. In addition, A2780 ovarian carcinoma cells undergo rapid apoptosis following exposure to CDK2 inhibitors of this class. Mechanism of action studies have confirmed that the phosphorylation of CDK2 substrates such as RB, histone H1, and DNA polymerase α (p70 subunit) is reduced in the presence of compound **14**. Further optimization led to compounds such as water soluble **45**, which possesses a favorable pharmacokinetic profile in mice and demonstrates significant antitumor activity in vivo in several murine and human models, including an engineered murine mammary tumor that overexpresses cyclin E, the coactivator of CDK2.

Introduction

The cyclin-dependent kinases (CDKs) are serine/threonine protein kinases, which are the driving force behind the cell cycle and cell proliferation.^{1,2} Individual CDKs perform distinct roles in cell cycle progression and can be classified as either G1, S, or G2/M phase enzymes. Uncontrolled proliferation is a hallmark of cancer cells, and misregulation of CDK function occurs with high frequency in many important solid tumors.³ CDK2 and CDK4 are of particular interest because their activities are frequently misregulated in a wide variety of human cancers. CDK2 activity is required for progression through G1 to the S phase of the cell cycle, and CDK2 is one of the key components of the G1 check-

point. Checkpoints serve to maintain the proper sequence of cell cycle events and allow the cell to respond to insults or to proliferative signals, while the loss of proper checkpoint control in cancer cells contributes to tumorigenesis.⁴ The CDK2 pathway influences tumorigenesis at the level of tumor suppressor function (e.g., p53, RB, and p27) and oncogene activation (cyclin E). Many reports have demonstrated that both the coactivator, cyclin E,⁵ and the inhibitor, p27,⁶ of CDK2 are either over- or underexpressed, respectively, in breast, colon, nonsmall cell lung, gastric, prostate, bladder, non-Hodgkin's lymphoma, ovarian, and other cancers. Their altered expression has been shown to correlate with increased CDK2 activity levels and poor overall survival.^{6,7} This observation makes CDK2 and its regulatory pathways compelling targets for the development of novel chemotherapeutic agents. During the past few years, a number of adenosine 5'-triphosphate (ATP) competitive small organic molecules^{8,9} as well as peptides¹⁰ have been reported in the literature as CDK inhibitors for the potential treatment of cancers. Currently, the nonselective CDK inhibitor flavopiridol is undergoing human clinical trials.¹¹

High throughput screening at Bristol-Myers Squibb for inhibitors of CDKs led to the identification of several new chemotypes. Among the most interesting of these was the 2-amino-5-thio-substituted thiazole **1** (Figure

* To whom correspondence should be addressed. Tel: (609)252-5181. Fax: (609)252-6601. E-mail: kyoung.kim@bms.com.

[†] Department of Oncology Chemistry, Bristol-Myers Squibb Pharmaceutical Research Institute.

[‡] Lexicon Pharmaceuticals, East Windsor, NJ.

[§] Department of Oncology Drug Discovery, Bristol-Myers Squibb Pharmaceutical Research Institute.

^{||} Department of New Leads Chemistry, Bristol-Myers Squibb Pharmaceutical Research Institute.

[⊥] Department of Structural Biology and Modeling, Bristol-Myers Squibb Pharmaceutical Research Institute.

[#] Memorial Sloan-Kettering Cancer Center, New York, NY.

[∇] Department of Metabolism and Pharmacokinetics, Bristol-Myers Squibb Pharmaceutical Research Institute.

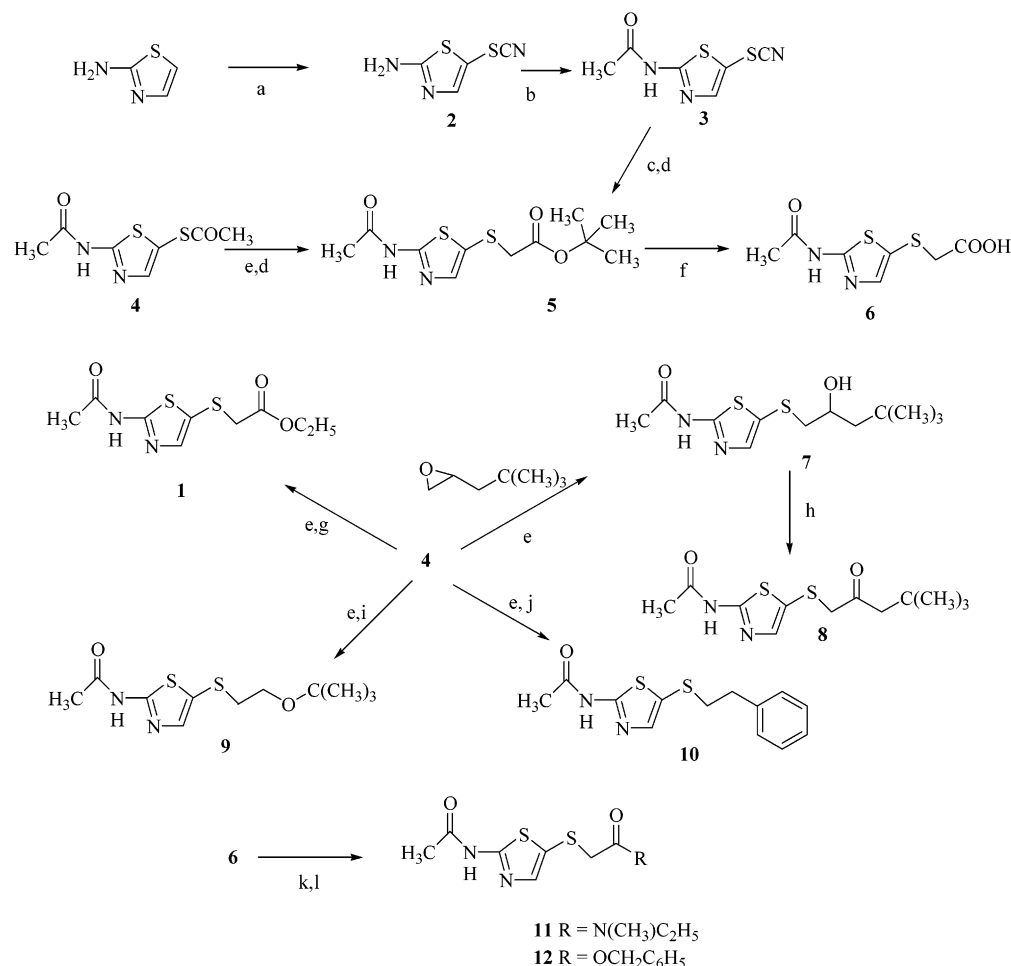
[○] Department of High Throughput Screening, Bristol-Myers Squibb Pharmaceutical Research Institute.

[^] Astra Zeneca R&D Boston Inc., Waltham, MA.

Compound	IC ₅₀ (μM)				
	CDK2/cyc E	CDK1/cyc B	CDK4/cyc D	PKC	PKA
1	0.17	1.9	23	>50	>50
Flavopiridol	0.33	0.03	0.15	15	>50

Figure 1.

1). While flavopiridol inhibits CDK1, CDK2, and CDK4 with minimal selectivity, the 2-amino-5-thiothiazole **1** is 10-fold selective vs CDK1 and 100-fold selective vs CDK4. The small molecular size combined with potency, structural simplicity, and modular synthesis made the compound **1** series a particularly interesting starting point for research. A robust structure–activity relationship (SAR) quickly evolved from both solution phase and solid phase chemistry, and X-ray crystallographic structures of the inhibitor–CDK2 complex provided insight into the binding of these molecules to the active site of

Scheme 1^a

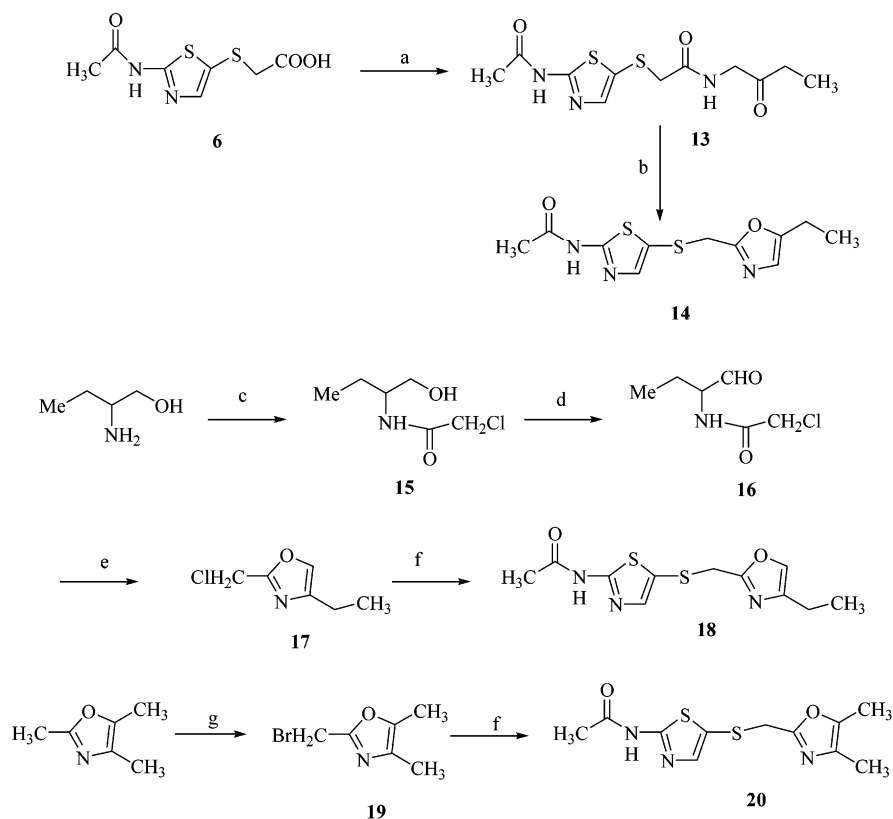
^a Conditions: (a) NaSCN, Br₂, MeOH. (b) Ac₂O, pyridine, CH₂Cl₂. (c) DTT, MeOH. (d) *tert*-Butyl bromoacetate. (e) KOtBu or NaOEt. (f) TFA. (g) Ethyl bromoacetate. (h) Dess–Martin periodinane. (i) 2-*tert*-Butoxyethyl methanesulfonate. (j) Phenethyl bromide. (k) HOBt, EDCI, ethylmethylamine. (l) Diethyl azodicarboxylate, PPh₃, benzyl alcohol.

CDK2. In this paper, we describe the discovery and optimization of aminothiazole-based CDK2 inhibitors, modeling studies based on X-ray crystallographic data, and *in vitro* and *in vivo* biological activities.

Chemistry

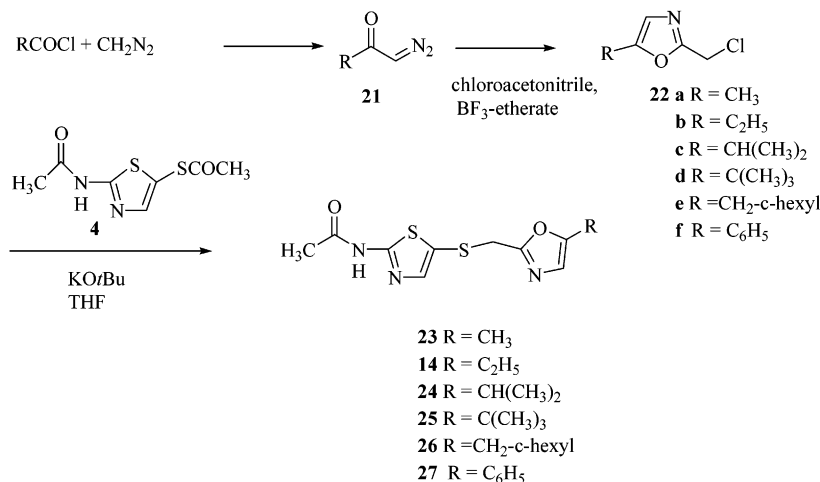
2-Amino-5-thiocyanatothiazole **2** was prepared by reacting 2-aminothiazole with sodium thiocyanate and bromine (Scheme 1).¹² Acylation of the 2-amino-5-thiocyanatothiazole with acetic anhydride gave key intermediate **3** on a multigram scale. Reduction of **3** by dithiothreitol (DTT) or sodium borohydride afforded the intermediate thiolate, which was alkylated *in situ* by an electrophile such as *tert*-butyl bromoacetate to give ester **5**. Alternatively, compound **5** could be obtained from commercially available 2-acetylthiothiazole **4**. In this case, treatment of **4** with alkoxide to cleave the thioester to the thiolate followed by reaction with *tert*-butyl bromoacetate provided **5** directly. This thiolate intermediate could be reacted with various electrophiles to produce analogues of **1** (**7–10**). Coupling of acid **6** with methylethylamine or benzyl alcohol provided amide **11** and benzyl ester **12**, respectively (Scheme 1).

The 5-ethyl-substituted oxazole analogue **14** was prepared from acid **6** by coupling with 1-amino-2-

Scheme 2^a

^a Conditions: (a) EDCl, HOBT, 1-amino-2-butanone, CH₂Cl₂. (b) Ac₂O, H₂SO₄, NaOAc. (c) Et₃N, chloroacetyl chloride. (d) Oxalyl chloride, Et₃N, DMSO. (e) POCl₃, 90 °C. (f) KOtBu, compound **4**. (g) NBS, benzoyl peroxide, 76 °C.

Scheme 3

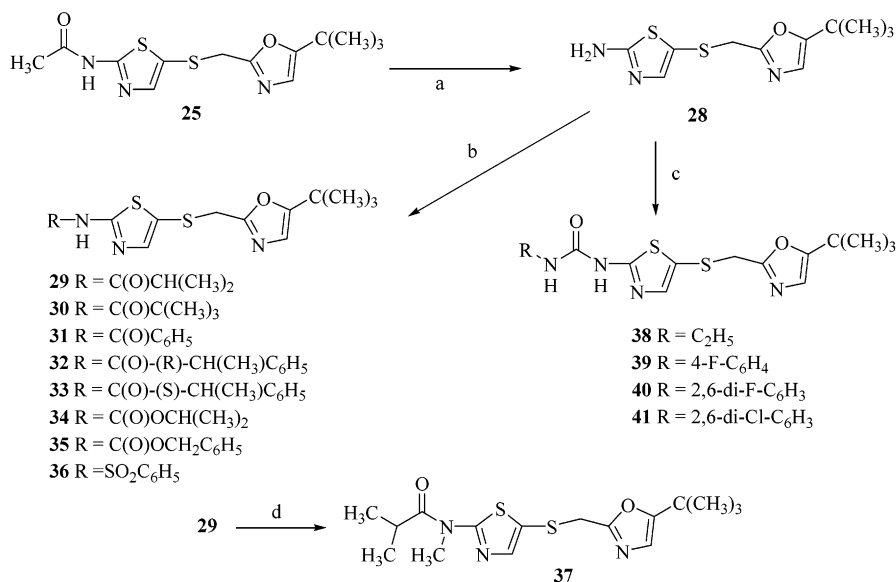


butanone followed by cyclodehydration of **13** using acetic anhydride and concentrated sulfuric acid (Scheme 2). To explore the SAR of the oxazole substitution, 4-ethyl-substituted oxazole regioisomer **18** and 4,5-disubstituted oxazole analogue **20** were prepared. Dehydrocyclization of aldehyde **16** with POCl₃ followed by the coupling of the resulting chloromethyl oxazole **17** with the thiolate intermediate from **4** provided regioisomer **18**. Treatment of 2,4,5-trimethyl oxazole with *N*-bromosuccinimide produced 2-bromomethyl oxazole **19**, which led to analogue **20** upon coupling with the thiolate from **4** (Scheme 2).

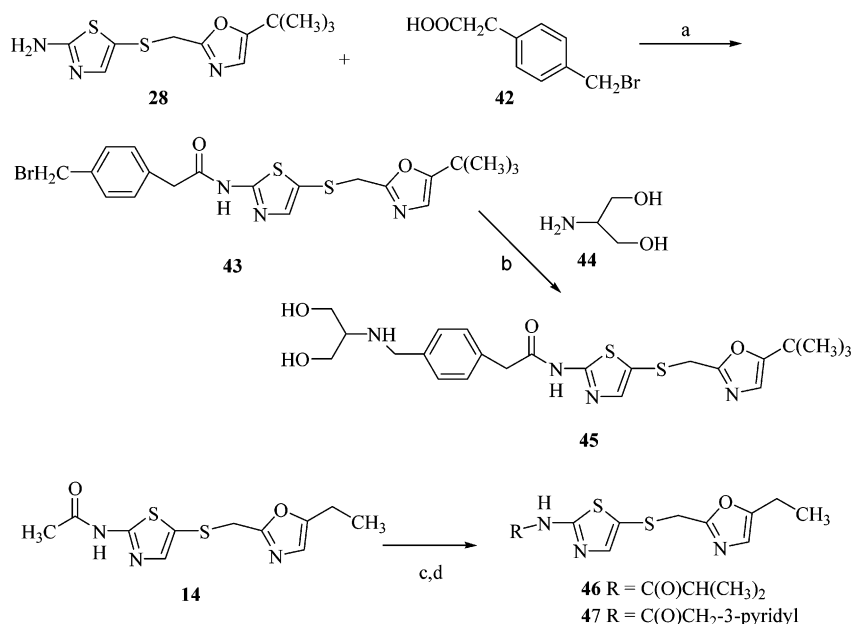
Alternatively, 2-chloromethyl oxazoles with various substituents at C-5, **22**, were prepared by the treatment

of diazoketone **21** with boron trifluoride etherate in the presence of chloroacetonitrile (Scheme 3).¹³ This methodology allowed the synthesis of oxazole analogues with various substituents at C-5 of the oxazole ring.

A wide variety of derivatives with different substituents on the C-2 amino group of the thiazole were easily prepared from amine **28** by reacting with activated acid derivatives to give amide analogues **29–33**, with chloroformates to give carbamates **34** and **35**, with sulfonyl chlorides to give sulfonamide **36**, and with isocyanates to give ureas **38–41** (Scheme 4). Methylation of the amide nitrogen of **29** was accomplished by reacting **29** with methyl iodide in the presence of potassium carbonate to obtain **37**.

Scheme 4^a

^a Conditions: (a) Aqueous NaOH, EtOH, 100 °C. (b) RCOCl, pyridine, or RCOOH, HOBt, EDCI, or ROCOCl, pyridine, DMAP, or PhSO₂Cl, pyridine. (c) RNCO, DMF, 55 °C. (d) MeI, K₂CO₃, DMF.

Scheme 5^a

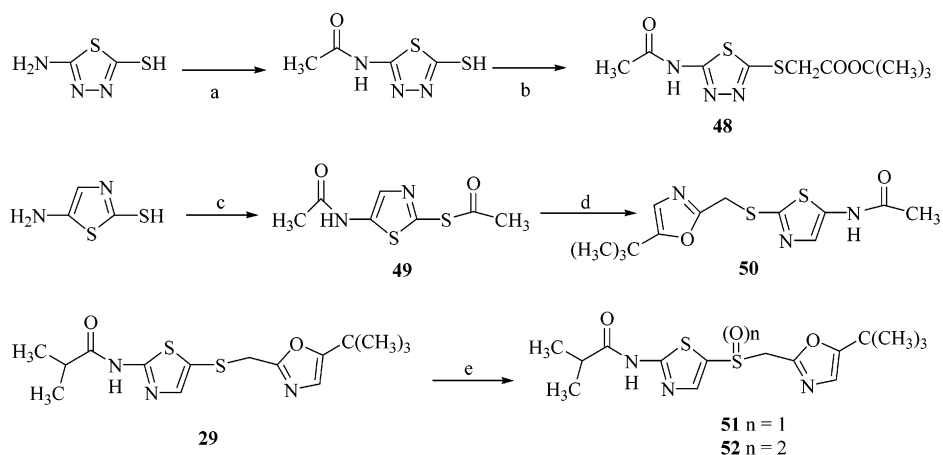
^a Conditions: (a) EDCI, CH₂Cl₂. (b) THF-DMF, room temperature. (c) Aqueous NaOH, EtOH, 100 °C. (d) RCOCl, pyridine, or RCOOH, HOBt, EDCI.

Acyl aminothiazoles with more polar functional groups were explored. The serinol functional group was introduced by the treatment of benzylbromo derivative **43** with serinol **44** to obtain **45**. Alternatively, the pyridyl-substituted 5-ethylthiazole analogue **47** was prepared by coupling with 3-pyridylacetic acid (Scheme 5).

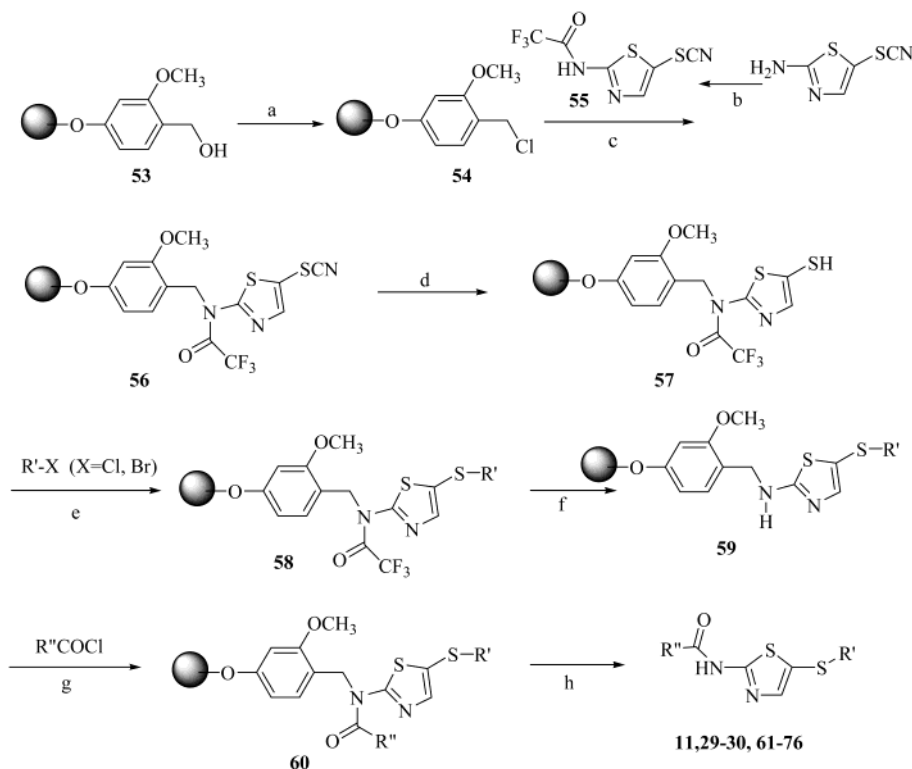
Alternative heterocycles and sulfur oxidation products were also studied (Scheme 6). Thiadiazole analogue **48** and the regioisomer of the 2-amino-5-thiothiazole nucleus, compound **50**, were synthesized from 2-mercapto-5-aminothiadiazole and 2-mercapto-5-aminothiazole,¹⁴ respectively. Oxidation of sulfide **29** with mCPBA provided sulfoxide **51** and sulfone **52**.

Libraries of 2-amino-5-thio-substituted thiazoles were prepared on solid phase using the methods shown in

Scheme 7. The synthesis was initiated by conversion of SASRIN resin **53**¹⁵ to its corresponding chloromethyl derivative **54** with triphosgene and PPh₃.¹⁶ After unsuccessful attempts to directly couple **2** to benzyl chloride resin **54**, the aminothiazole was acylated with trifluoroacetic anhydride to give **55**, which was alkylated with benzyl chloride resin **54** in the presence of ^tPr₂N⁺Et to form a resin-bound thiocyanate **56**. Thiocyanate **56** was then reduced to a resin-bound thiol **57** with DTT. The resulting resin-bound thiol **57** was alkylated with a variety of chlorides or bromides in the presence of DBU to obtain a series of analogues **58**. Deprotection of the trifluoroacetyl group using sodium borohydride in ethanol followed by acylation of the secondary amine of **59** provided amide **60** with a variety of R'' groups. Cleaving

Scheme 6^a

^a Conditions: (a) Ac₂O, pyridine. (b) *tert*-Butyl bromoacetate. (c) CH₃COCl, pyridine. (d) KOtBu, compound **22d**, THF. (e) mCPBA, CH₂Cl₂.

Scheme 7^a

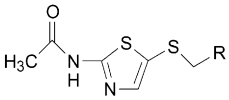
^a Conditions: (a) Triphosgene, PPh₃, CH₂Cl₂. (b) TFAA, 2,6-lutidine. (c) *i*-Pr₂EtN, CH₂Cl₂. (d) DTT, THF/MeOH. (e) DBU, DMF, 70 °C. (f) NaBH₄, EtOH/THF. (g) *i*-Pr₂EtN, CH₂Cl₂, 0 °C to room temperature. (h) 50% TFA/CH₂Cl₂.

the product from solid support with 50% trifluoroacetic acid (TFA)/CH₂Cl₂ provided the final products, some of which are shown in Table 7.

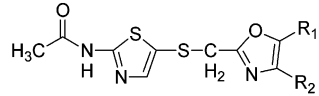
SAR and Structural Studies

The initial screening hit compound **1** is a relatively selective inhibitor of CDK2 (Table 1). The bulkier *tert*-butyl ester group of **5** increases the activity as compared to the original ethyl ester **1**, but there appears to be a limit to the allowable size of the ester as benzyl ester **12** shows reduced activity (**5** vs **12**). A simple hydrophobic substituent as in **10** has diminished activity, which implies the possible involvement of the ester function in hydrogen bonding with the protein in the binding site. However, potential hydrogen-bonding ac-

ceptors such as alcohol **7**, ketone **8**, ether **9**, and amide **11** exhibit only weak activity, at best. The combination of a finely tuned hydrophobic moiety and a hydrogen-bonding acceptor within the ester moiety appears to be needed for good inhibitory activity although we still cannot rule out stabilization of the bioactive conformation by the ester or its involvement in other interactions. Despite its potent CDK2 inhibitory activity, compound **1** lacks cell activity (IC₅₀ > 25 μM) in a cell proliferation assay (ovarian tumor cell line A2780). We hypothesized that this is due to metabolism of the ester to the carboxylic acid **6** (Table 1), which is completely devoid of CDK2 inhibitory activity. With the metabolic liability of the ester function in mind, a metabolically stable ester surrogate¹⁷ was sought to replace the ester in **1**.

Table 1. SAR of Thiomethylene Substitution


compd no.	R	IC ₅₀ (μM)		
		CDK2/ cyc E	CDK1/ cyc B1	CDK4/ cyc D1
1	COOC ₂ H ₅	0.17	1.87	23.03
5	COOC(CH ₃) ₃	0.05	0.44	5.38
6	COOH	>25		
7	CH(OH)CH ₂ C(CH ₃) ₃	2.81		
8	C(O)CH ₂ C(CH ₃) ₃	1.84		
9	CH ₂ OC(CH ₃) ₃	1.74		
10	CH ₂ C ₆ H ₅	12.58		
11	C(O)N(CH ₃)C ₂ H ₅	>25		
12	COOCH ₂ C ₆ H ₅	0.34	2.38	19.06

Table 2. SAR of Oxazole Substitution


compd no.	R ₁	R ₂	IC ₅₀ (μM)			
			CDK2/ cyc E	CDK1/ cyc B1	CDK4/ cyc D1	cytotox A2780
14	C ₂ H ₅	H	0.02	0.30	2.25	1.40
18	H	C ₂ H ₅	0.20			
20	CH ₃	CH ₃	0.36			
23	CH ₃	H	0.09		5.16	
24	CH(CH ₃) ₂	H	0.006	0.06	1.07	0.20
25	C(CH ₃) ₃	H	0.005	0.04	0.69	0.05
26	CH ₂ - <i>c</i> -hexyl	H	0.004	0.03	0.64	1.54
27	C ₆ H ₅	H	0.35		4.51	

This led to key 5-ethyloxazole-substituted thiazole **14**. The oxazole **14**, which is metabolically stable against esterases, maintained CDK2 selectivity and displayed increased kinase inhibitory potency (**14** vs **1**) as well as potent antiproliferative activity with an IC₅₀ of 1.4 μM in the 72 h ovarian cancer cell A2780 proliferation assay (Table 2).

The solid state structure of CDK2 with compound **5** bound in the ATP binding site was determined by single-crystal X-ray diffraction (Figure 2). Interestingly, the thiazole ester **5** adopts a folded conformation in the CDK2-bound complex, while the X-ray structure of **5** alone reveals an extended conformation (data not shown). In this folded conformation, as in all of the subsequent structures of the 2-amino-5-thioalkyl-substituted thiazoles bound to CDK2, a pair of reciprocal hydrogen bonds is formed in the CDK2 hinge region of the ATP binding site between the 2-amino hydrogen and the carbonyl of Leu83, as well as the 3-nitrogen of the aminothiazole ring and the NH of Leu83. The thiomethylene moiety occupies a hydrophobic pocket formed by Ala31, Val64, Phe80, and Ala144 of CDK2, and the alkyl group of the ester resides in a region containing hydrophobic residues such as Val18, Leu134, and the C_α and C_β atoms of Asn132. In addition, the 2-amide carbonyl oxygen of **5** forms a hydrogen bond with a water molecule, an interaction that was not always found in the structures of related analogues.

Although we anticipated that the ester carbonyl or oxazole heteroatom(s) would be involved as a hydrogen-bonding acceptor with the nearby residue Lys33 of the

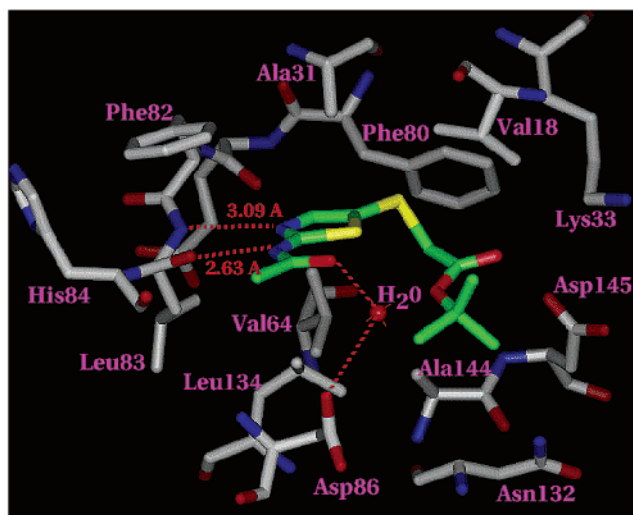


Figure 2. ATP binding site residues of the X-ray structure of CDK2 in complex with compound **5**. Hydrogen-bonding interactions are shown. The oxygen atoms are colored red, nitrogen atoms are colored blue, protein carbon atoms are colored gray, and ligand carbon atoms are colored green.

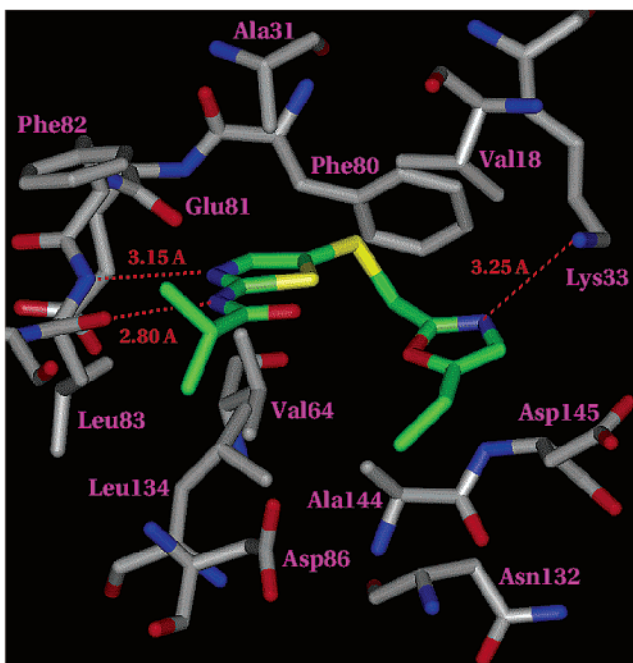


Figure 3. ATP binding site residues of the X-ray structure of CDK2 in complex with compound **46**.

ATP binding site, it is observed that in most of the solid state X-ray structures the density of the Lys33 side chain was insufficient to assign its position unambiguously. The ester carbonyl oxygen of **5** is directed toward the Lys33 side chain but is 4.4 Å from the side chain terminal amino nitrogen and 3.4 Å from the side chain C_ε. In only a few cases, such as the CDK2 complex with **46**, is the oxazole ring nitrogen and the terminal side chain amino nitrogen of Lys33 within a reasonable hydrogen-bonding distance (3.25 Å) as shown in Figure 3. For most of the structures, in which the analogue binds in a folded conformation, the geometry reveals an efficient packing of the oxazole ring with residues such as Val18 and/or the hydrocarbon portion of the Lys33 side chain. The 5-oxazole substituent makes similar interactions with CDK2 as shown above for the *tert*-

Table 3. SAR of 2-Amino Substitution

compd no.	R ₁	R ₂	IC ₅₀ (μM)			
			CDK2/ cyc E	CDK1/ cyc B1	CDK4/ cyc D1	cytotox A2780
25	C(O)CH ₃	H	0.005	0.04	0.69	0.05
29	C(O)CH(CH ₃) ₂	H	0.005	0.03	0.03	0.05
30	C(O)C(CH ₃) ₃	H	0.017	0.09	3.48	0.25
31	C(O)C ₆ H ₅	H	0.026		0.96	0.84
32	C(O)-(R)-CH(CH ₃)C ₆ H ₅	H	0.006		3.13	0.9
33	C(O)-(S)-CH(CH ₃)C ₆ H ₅	H	0.06			
34	C(O)OCH(CH ₃) ₂	H	0.025	0.018	2.99	0.64
35	C(O)OCH ₂ C ₆ H ₅	H	0.15			1.04
36	SO ₂ C ₆ H ₅	H	4.28			2.86
37	C(O)CH(CH ₃) ₂	CH ₃	>25			
38	C(O)NHC ₂ H ₅	H	0.05			0.12
39	C(O)NH-(4-F)-C ₆ H ₅	H	0.011	0.019	0.90	0.90
40	C(O)NH-(2,6-di-F)-C ₆ H ₃	H	0.002	0.010	0.39	0.24
41	C(O)NH-(2,6-di-Cl)-C ₆ H ₃	H	0.003	0.03	>1	1.5
45	C(O)CH ₂ -(4-CH ₂ NHCH(CH ₂ OH) ₂)-C ₆ H ₄	H	0.003	0.03	0.10	0.03

butyl group of ester **5**. While the 5-substituent of the oxazole interacts favorably with hydrophobic residues in a location that preferably accommodates a sizable group, the C-4 position of the oxazole points toward buried residues such as Lys33 and Asp145 of the ATP binding site. Therefore, anything larger than a hydrogen atom would be disruptive to binding. This is consistent with the diminished activity of regioisomer 4-ethyloxazole **18** and 4,5-dimethyl-substituted oxazole **20** as compared to **14** (Table 2).

Increasing the bulk of the 5-oxazole substituent by incorporating a branched sp³ carbon center increases potency in vitro (**24–26** vs **23**) against CDK2/cyclin E (Table 2). However, substitution by a phenyl ring (**27**) decreases activity. Apparently, the 5-oxazole substituent binding pocket can accommodate a large substituent as evidenced by the good activity of **26**. Modeling studies of **27** in the active site of CDK2 reveal that in the folded conformation both the 2-amide carbonyl oxygen of the thiazole and the backbone carbonyl oxygen of Gln131 point toward the C-5 phenyl of the oxazole. The interaction of the π system of the C-5 phenyl with the carbonyl oxygens of the 2-amide group of the thiazole or of Gln132 would be unfavorable. In addition, because the phenyl ring is more rigid, it may not be able to adjust to fit the enzyme pocket as productively as the analogues with more flexible sp³-hybridized carbons at the C-5 position of the oxazole.

Because the 5-*tert*-butyl oxazole appears nearly optimal in its activity against CDK2/cyclin E and in the A2780 cell proliferation assay, most of the SAR that is discussed in this paper is restricted to analogues in which this moiety is held constant. Using solution phase parallel synthesis as well as individual compound synthesis, we rapidly prepared a series of 5-*tert*-butyl-oxazolymethylthio thiazoles that further explored the SAR of the 2-amino substitution.

While there are clear differences in the enzyme selectivity and cell activity among amides and carbamates (**25** and **29–35**), these substitutions are broadly active against CDK2/cyclin E (Table 3). Carbamates (**34** and **35**) are generally less potent inhibitors of the CDK2/cyclin E complex than are the amides. Interestingly,

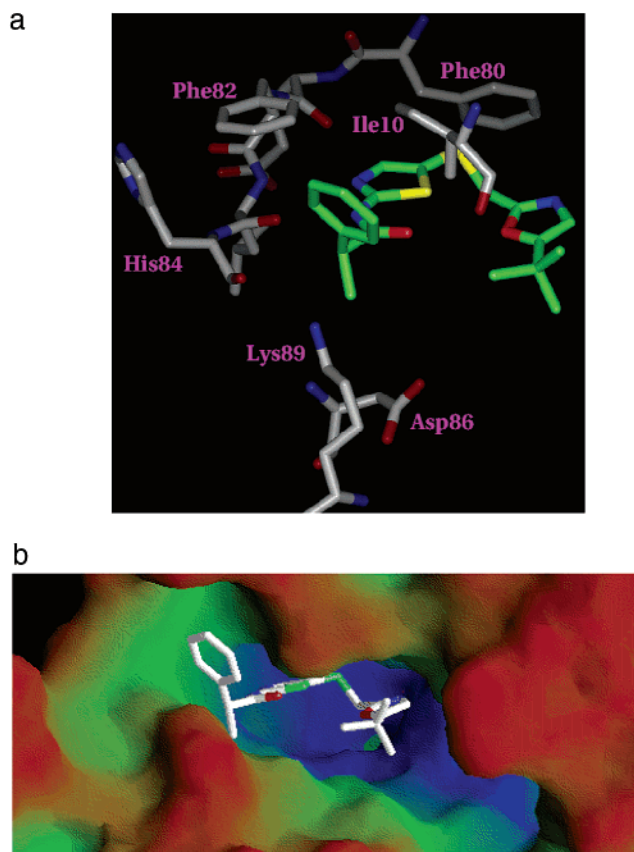


Figure 4. (a) ATP binding site residues of the X-ray structure of CDK2 in complex with compound **32**. (b) The ATP binding site of the X-ray structure of CDK2 (shown as a solid molecular surface) in complex with compound **32**. The surface of CDK2 is colored according to elevation, i.e., blue indicates deepest pockets, green indicates more shallow pockets, and orange indicates peaks.

carbamate **34** lost the selectivity of CDK2 inhibitory activity over CDK1. It is noteworthy that there is a 10-fold activity difference between the two stereoisomers of **32** and **33**. Figure 4a,b shows the solid state structure of **32** bound to the active site of CDK2. Modeling studies of (*S*)-isomer **33** in the X-ray structure of CDK2 (not shown) revealed that the phenyl ring of the 2-amino

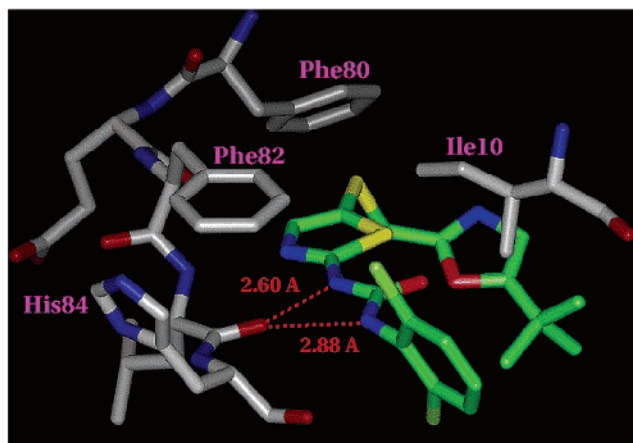


Figure 5. ATP binding site residues of an X-ray structure of CDK2 in complex with compound **41**.

substituent would likely form significant steric contacts with the side chains of Lys89 and Asp86, the latter residue being involved in an intramolecular hydrogen bond with the backbone amino nitrogen of Lys89, an interaction found in all of the in-house crystal structures. Furthermore, the favorable interactions of the phenyl ring with Phe82 and Ile10 observed with the (*R*)-isomer **32** would be lost with the (*S*)-isomer, thereby providing a possible explanation for the decrease in activity of (*S*)-isomer **33**.

A sulfonamide **36** is much less active, and consistent with the structural information in Figure 3, *N*-methylation of the 2-amide (**37**) destroys activity in vitro. Therefore, the hydrogen-bonding donor NH of the amide (and the NH(s) of the urea, see below) to Leu83 is essential to potent activity against CDK2/cyclin E (**29** vs **37**).

Phenyl-substituted ureas (**39–41**) are more potent inhibitors than the simple ethyl urea **38**. The X-ray structure of the complex of CDK2 and the 2,6-dichlorophenyl analogue **41** reveals that the phenyl ring of **41** interacts favorably with the side chains of Ile10 and Phe82, which may explain why phenyl-substituted ureas are more potent inhibitors than the simple ethyl urea (see Figure 5). The diortho substitution on the phenyl ring helps orient the ring out-of-plane with the urea group in such a way that it optimally interacts with Ile10. In addition, both urea NHs are within hydrogen-bonding distance (2.60 and 2.88 Å) to the carbonyl of Leu83. The X-ray structure complexes of CDK2 and **41** with and without cyclin A were obtained (Figure 6a,b). It is observed that the binding mode and ligand conformation are virtually identical in both complexes. However, the T loop of CDK2 is in different locations in the two structures. The T loop is oriented further away from the ATP binding site in the ternary complex of CDK2, **41**, and cyclin A than is found in the complex without cyclin A. This observation is similar to the findings of Pavletich et al.¹⁸

As shown in the X-ray structure of Figure 4b, the 2-amide side chain of the thiazole **32** in the binding pocket of CDK2 points toward the solvent-exposed region. However, because the portion of the 2-substituent closest to the thiazole nucleus is still within the binding site and able to interact with the protein, functional group changes near the 2-amino tether may

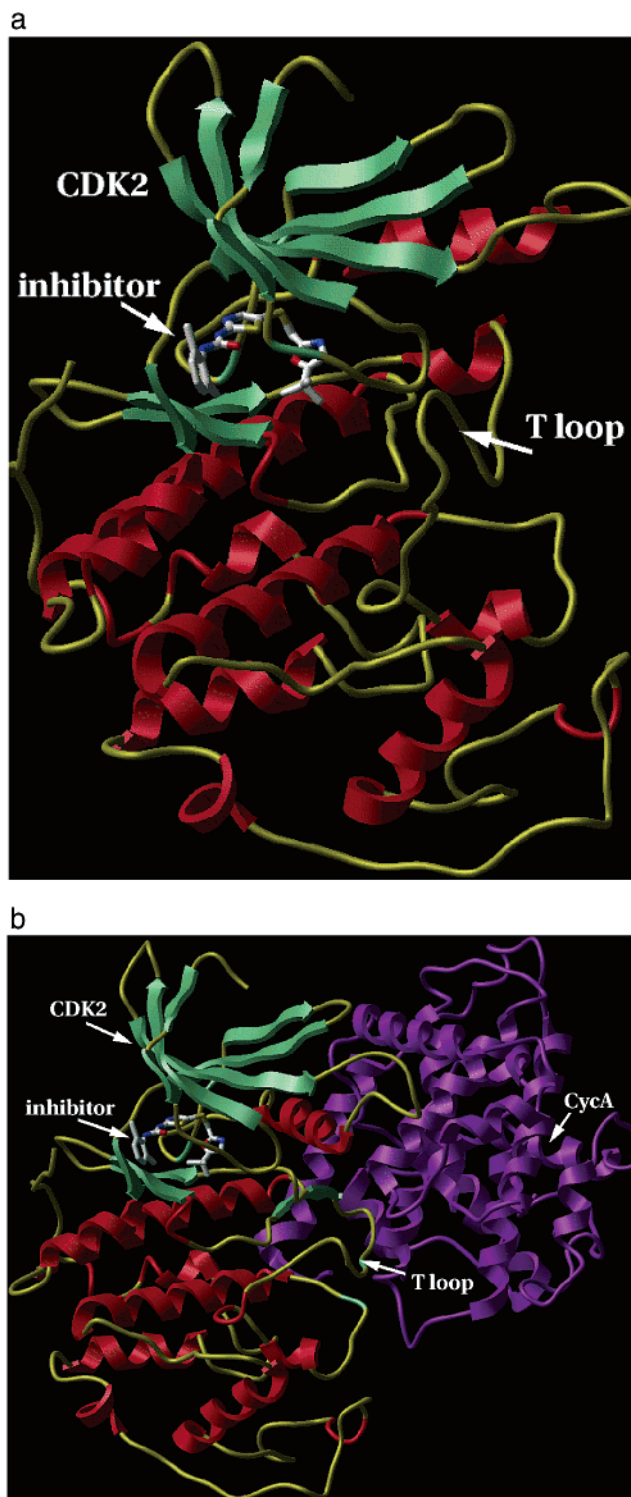
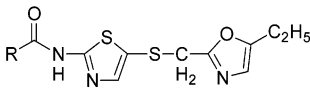
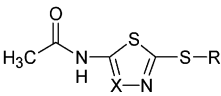


Figure 6. (a) Schematic drawing of the CDK2–**41** complex. CDK2 is shown in a ribbon representation with the α -helices in red, β -sheets in green, and loops in yellow. Compound **41** is shown in stick representation. (b) The CDK2–**41**–cyclin A ternary complex. Cyclin A is colored purple.

correlate with differences in activity. On the other hand, as the 2-amino substituent extends further away from the thiazole ring and toward solvent, the interactions with the CDK2 become less likely. In as much as the 2-amino substituent is directed toward the solvent-exposed hinge region, we felt that substitution at the 2-amino position would be key for optimizing the physical and pharmacokinetic properties of these molecules

Table 4. CDK Activity Data of the Ethyloxazole Analogue


compd no.	R	IC ₅₀ (μM)			
		CDK2/ cyc E	CDK1/ cyc B1	CDK4/ cyc D1	cytotox A2780
46	CH(CH ₃) ₂	0.005	0.060	1.07	0.20
47	CH ₂ -3-pyridyl	0.005	0.08	1.09	0.24

Table 5. CDK Activity Data of the Analogue


R₁ = CH₂COOC(CH₃)₃
R₂ = H₂C-C(CH₃)₃-oxazole

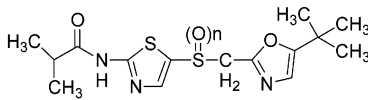
compd no.	X	R	CDK2/cyc E IC ₅₀ (μM)
48	N	R ₁	>25
50	CH	R ₂	>25

while still retaining good CDK2 inhibitory activity. With these thoughts in mind, a polar amino alcohol group as well as a pyridyl moiety were introduced as in **45** and **47** to improve the aqueous solubility. In concordance with our expectations, the more water soluble, yet higher molecular weight compound **45** retained potent activity in both CDK2/cyclin E enzyme and cell proliferation assays. Pyridyl-substituted 5-ethyloxazole analogue **47** also exhibited potent inhibitory activity against CDK2/cyclin E, but it was less active than amino alcohol-substituted 5-*tert*-butyloxazole analogue **45** in the cytotoxic assay (Tables 3 and 4).

In an effort to understand the binding requirements for activity against CDK2/cyclin E, several compounds were prepared that incorporate modifications of the central thio-aminothiazole ring (Table 5). Incorporation of an additional nitrogen into the heterocycle as in thiodiazole **48** or moving the position of the ring nitrogen of the aminothiazole (**50**) led to a complete loss of activity against the enzyme. Modeling studies suggest that substitution of the thiazole CH with N introduces an unfavorable N...O lone pair electron repulsion with the carbonyl oxygen of Glu81. Furthermore, a favorable interaction found with the parent aminothiazole ring, which participates in an aromatic CH...O=C interaction with the carbonyl oxygen of Glu81, an interaction also observed with CDK2 complexes of other chemotypes,¹⁹ is absent in **48**. The inactivity of **50** can be explained by the observations from the solid state structure that the 3-nitrogen of the parent thiazole ring participates in a critical hydrogen bond with the amide NH of Leu83.

Potential oxidative metabolism of the sulfur atom led to the exploration of sulfoxide **51** and sulfone **52**. These oxidized compounds show diminished activity in vitro (Table 6). However, studies of the oxidative metabolism of the sulfur atom in vivo indicated that sulfur oxidation was not a major problem since the amount of oxidative metabolism of sulfur was minimal.

Only a few examples from the solid phase synthesis are shown in Table 7. As seen in this table, the 5-alkyloxazoles were optimal as other heterocycles (e.g., **61**, **64–66**, etc.) were much less active.

Table 6. SAR of the Sulfur Oxidation Analogues


compd no.	n	IC ₅₀ (μM)		
		CDK2/ cyc E	CDK1/ cyc B1	CDK4/ cyc D1
29	0	0.005	0.03	0.90
51	1	0.14	0.14	>25
52	2	0.25	>0.25	

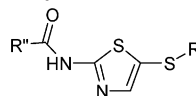
Biological Evaluation

Kinase Selectivity. To establish that compounds from this series were specific for the CDK class of serine/threonine protein kinases, a panel of assays was established. Using a diverse set of kinase proteins, we were able to track changes in the structures that conferred specificity for CDKs vs a number of unrelated serine/threonine kinases, such as protein kinase C (PKC) family members, as well as nonreceptor and receptor tyrosine kinases such as Lck, EMT, Zap70, and Her family and IGF-1 enzymes. More importantly, assays for CDK1 and CDK4 allowed us to establish which compounds were selective for CDK2 relative to other close family members. As can be seen in Table 8, compounds such as the 5-ethyloxazole- or 5-*tert*-butyloxazole-substituted thiazoles **14** and **45** were relatively selective for CDK2, being 10-fold more potent against this enzyme than CDK1/cyclin B complex. The CDK2 inhibitory activity observed was superior to that of the clinical compound flavopiridol, which was less selective among all CDK complex activities studied, as well as inhibiting some PKC family members. Improvements in aqueous solubility by introduction of the polar moiety in **45** were compatible with improving potency and retaining selectivity for CDK2. This compound was 10- and 30-fold selective for CDK2 vs CDK1 and CDK4 and 3–5 orders of magnitude more potent against CDK2 than all other non-CDKs tested (Table 8).

CDK Substrate Phosphorylation. Confirmation that these compounds were inhibiting CDK2 enzyme activity in cells was obtained through examination of CDK substrate phosphorylation states. Actively proliferating A2780 ovarian carcinoma cells were treated with ³²P-orthophosphate in the presence or absence of 3 μM **14**. Subsequent immunoprecipitation of the CDK substrates RB, histone H1, and DNA polymerase α with specific antibodies showed reduced labeling with ³²P in the presence of compound **14**, as compared to untreated cells (Figure 7). In each case, there was an obvious reduction in the level of phosphorylation, suggesting that CDK2 function was inhibited in the cellular context. Equal loading of substrate was verified by parallel immunoprecipitation followed by western blot with the same antibody (data not shown).

Cell Cycle Analysis. Treatment of A2780 cells with CDK2 inhibitors, as described in the Experimental Section, resulted in an altered cell cycle distribution relative to untreated cells. The cell cycle effects of **14** and **47** are compared to flavopiridol at equipotent concentrations (determined in the 72 h cell proliferation assay with A2780 cells) in Table 9. It is clear that exposure to either compound **14** or compound **47** results

Table 7. CDK Activity Data of the Analogue from Solid Phase Synthesis



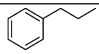
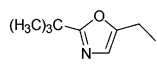
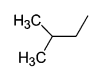
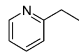
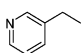
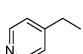
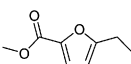
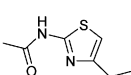
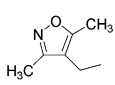
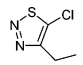
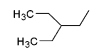
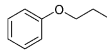
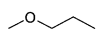
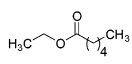
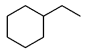
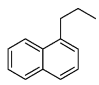
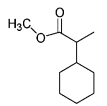
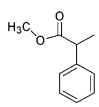
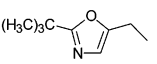
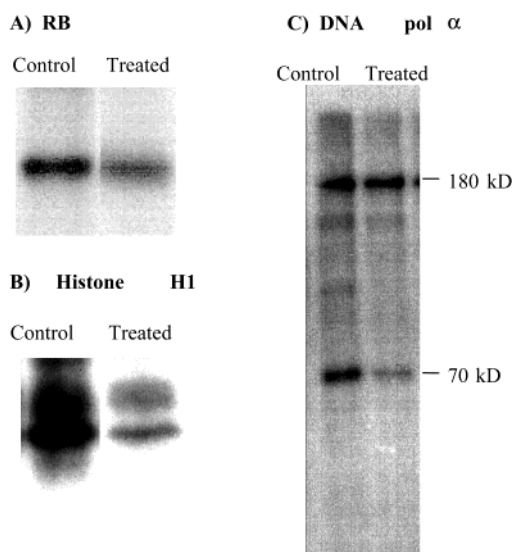
Compd #	R'	R''	CDK2/cyc E IC ₅₀ (μM)	Purity %	Yield %
11		CH ₃	>1	87	35
30		C(CH ₃) ₃	0.017	97	39
57		CH ₃	>1	75	34
61		CH ₃	>1	88	58
62		CH ₃	0.68	91	10
63		CH ₃	>1	97	12
64		CH ₃	>1	78	41
65		CH ₃	>1	82	60
66		CH ₃	>1	91	57
67		CH ₃	>1	86	50
68		CH ₃	>1	80	32
69		CH ₃	>1	84	32
70		CH ₃	>1	78	39
71		CH ₃	>1	87	34
72		CH ₃	>1	80	25
73		CH ₃	>1	82	33
74		CH ₃	>1	89	20
75		CH ₃	>1	96	5
76		CH ₂ C ₆ H ₅	0.003	98	28

Table 8. In Vitro Kinase Inhibition, IC₅₀ (nM)

protein kinase	flavopiridol	14	45
CDK1/cyclin B	30	297	30
CDK2/cyclin E	330	21	3
CDK4/cyclin D1	150	2250	102
PKC α	2800		>45 000
PKC β	>45 000		>45 000
PKC δ	890		45 000
PKC ϵ	480		5600
PKC ζ	>45 000		35 000
IKK	>100 000		28 000
EMT	14 850	>10 000	29 000
Lck	11 000		>40 000
ZAP70	>50 000		>50 000
Her1	7600		>25 000
Her2	15 800	>25 000	>25 000
IGFR	13 000	>25 000	24 000

**Figure 7.** Immunoprecipitation of CDK substrate proteins following ³²P-orthophosphate labeling.**Table 9.** Cell Cycle Analysis of A2780 Cells Treated with CDK Inhibitors (IC Values against CDK2/cyc E)

cell cycle position	control	14		47		flavopiridol	
		IC ₅₀ (20 nM)	IC ₉₀ (295 nM)	IC ₅₀ (5 nM)	IC ₉₀ (29 nM)	IC ₅₀ (330 nM)	IC ₉₀ (2980 nM)
G1	63	58	62	71	50	60	61
S	16	11	6	7	7	16	12
G2/M	18	29	25	20	18	23	25
sub-G1	3	2	7	2	25	1	2
apoptotic	3	6	16	4	69	1	9

in a clear decrease in the S phase cell population as well as a substantial increase in apoptotic cells (measured as either sub-G1 or <2 N DNA content determined by propidium iodide staining or as tunnel positive cells). Response to flavopiridol is more modest after 24 h of compound exposure. While there is a significant level of apoptosis induced, there is a less dramatic impact on the S phase cell population (Table 9). It is known that the CDK2 peptide inhibitors also induce the apoptosis of the transformed cells.¹⁰

In Vitro Cytotoxicity. Flavopiridol and many thiazole series CDK inhibitors demonstrated potent in vitro cytotoxicity against the ovarian tumor cell line A2780/DDP-S with IC₅₀ values of 0.05–1.5 μ M (Tables 2–4). In addition, some compounds were tested against a cell line panel consisting of mostly human tumors but also

Table 10. Intraperitoneal Dose in Mice

compd	dose (mg/kg)	dose (μ mol/kg)	C _{max} (μ M)	T _{max} (h)	AUC _{tot} (μ M·h)	T _{1/2} (h)	MRT (h)
flavopiridol	50	114	6.9	0.5	13.2	1.1	2.0
45	10	18	0.8	1	2.7	1.8	2.9
47	36	100	40	0.5	23	1.1	0.8

Table 11. Compound 45: IV and Oral Dose in Mice

	IV dose	oral (PO) dose
dose (mg/kg)	10	10
dose (nmol/kg)	18 971	18 971
C _{max} (nM)	8272	634.6
T _{max} (h)	0.08	0.33
AUC _{tot} (nM·h)	4984	1201
T _{1/2} (h)	2.2	1.4
MRT (h)	1.8	4.1
clearance (mL/min/kg)	67	
V _{ss} (L/kg)	6.9	
bioavailability (%)		24

human normal fibroblast cells, as well as mouse tumor and fibroblast cells and bovine normal endothelial cells. The data are expressed as IC₅₀ values and visually as a mean bar graph, which is derived from the IC₅₀ results (Figure 8). In a mean bar graph, bars to the right indicate cell lines that are more sensitive than the mean while bars that project to the left represent cell lines that are less sensitive than the mean.²⁰ As shown in Figure 8, the cell panel mean IC₅₀ value for flavopiridol was 0.055 and 1.24 μ M for compound 14, which was chosen as a representative example. Examination of the individual IC₅₀ values or the mean bar graph pattern indicates that these compounds have potent cytotoxic activity against a wide variety of cell types (ovarian, breast, prostate, colon, lung, and leukemia) with a modest difference (7-fold) between the most sensitive and the most resistant cell lines. Interestingly, a similar pattern of cell line selectivity is observed between these two compounds even though compound 14 is a more selective CDK2 inhibitor than flavopiridol.

Pharmacokinetics and Metabolism in Mice. Pharmacokinetic parameters of flavopiridol, 45, and 47 in mice after intraperitoneal dosing are summarized in Table 10. The half-life and the mean residence time (MRT) of 45 after ip dosing were longer than 47 and flavopiridol. Compound 45 was also administered in a second study by the IV and oral routes at a dose of 10 mg/kg; the estimated half-life and the MRT were 2.2 and 1.8 h, respectively, with a large V_{ss} (Table 11 and Figure 9). The oral bioavailability of 45 is 24%. Human serum protein binding for 45 and 47 was 78 and 82%, respectively, and the extent of binding of 45 to plasma protein was similar in human (78%) and mouse (79%), while the protein binding of flavopiridol was found to be 91 and 63%, respectively. The rate of oxidation of 45 in vitro in mouse and human microsomes was moderate (Table 12).

In Vivo Antitumor Activity. To determine the in vivo antitumor effects of CDK inhibition, compounds were evaluated against a panel of four tumor models including the P388 murine leukemia model, a murine mammary carcinoma originated from a strain of transgenic mice overexpressing cyclin E (Br-CycE),²¹ human ovarian carcinoma (A2780), and human squamous cell carcinoma (A431). Figure 10 shows the effects of 45 in the ip/ip P388 leukemia model. Drug treatment was

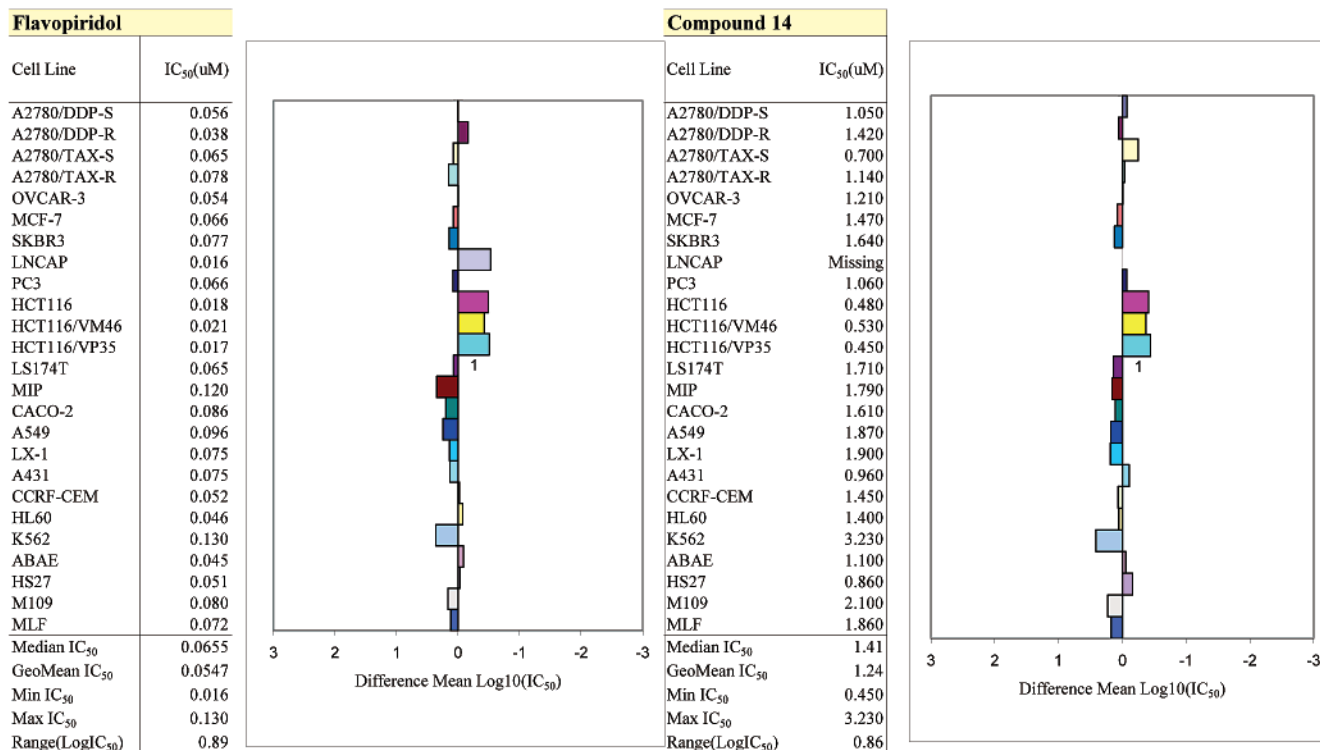


Figure 8. In vitro cytotoxicity of CDK inhibitors against a panel of tumor and normal cell lines. IC₅₀ values were determined after 72 h drug exposure.

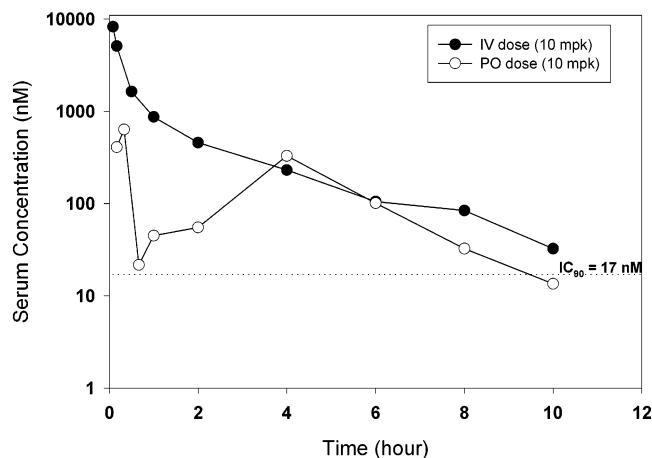


Figure 9. Plasma concentration vs time profiles of **45** in mice after IV and oral dosing.

Table 12. In Vitro Data of Flavopiridol, **45**, and **47**

compd	% serum protein binding		metabolic rate (nmol/min/mg protein)	
	human	mouse	human	mouse
flavopiridol	91	63	0.07	0.03
45	78	79	0.21	0.22
47	82			

initiated on day 1, ip, every day for 7 days (q1d \times 7). Treatment with compound **45** at its maximum tolerated dose (MTD) of 32 mg/kg/inj resulted in a significant increase of lifespan (%T/C = 140) (Figure 10 and Table 13). Both flavopiridol and **47** were inactive at their MTDs (6 and 120 mpk) in this model, yielding %T/C values of 110 and 115%, respectively (Table 13).

Compound **45** was highly active against the human A2780 ovarian carcinoma implanted sc in nude mice,

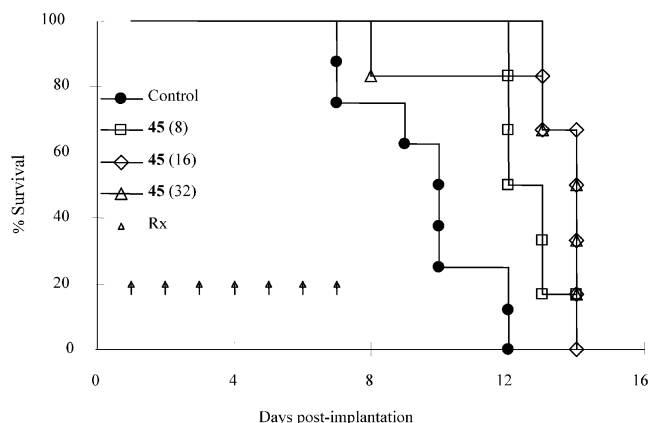


Figure 10. Effects of compound **45** treatment on the lifespan of mice inoculated ip with the leukemia P388. Mice received treatment daily for 7 consecutive days (8, 16, and 32 mg/kg/inj), beginning 1 day posttumor inoculation. Each symbol represents an individual mouse, each treatment group consisted of six mice, and the control group contained eight mice.

Table 13. In Vivo Antitumor Activity against P388 Murine Leukemia

compd	dose (mg/kg) (MTD)	route/schedule	%T/C
flavopiridol	7.5	ip/qdx7	110
45	32	ip/qdx7	140
47	120	ip/qdx7	115

producing 3.3 log cell kill (LCK) at its MTD (36 mpk, ip, qd \times 8) (Figure 11). In comparison, both flavopiridol and **47** were considerably less active, producing only 1.5 and 0.4 LCK, respectively, in this model at their MTDs (Table 14).

Compound **45** demonstrated antitumor activity in two other tumor models. In the Br-CycE mammary carcinoma, it yielded 1.1 LCK at its MTD (24 mpk, ip, q1d

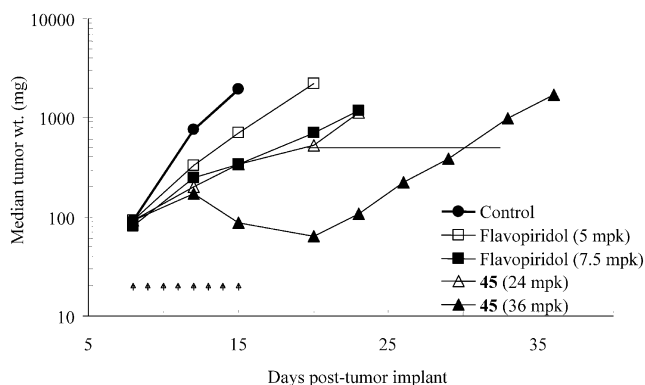


Figure 11. Comparative antitumor activity of flavopiridol and compound **45** on the human ovarian carcinoma A2780 grown in nude mice.

Table 14. In Vivo Antitumor Activity against A2780 Human Ovarian Carcinoma

compd	dose (mg/kg) (MTD)	route/schedule	LCK
flavopiridol	7.5	ip/qdx8	0.6–1.5
45	36	ip/qdx8	3.3
47	75	ip/2qdx9	0.4

× 8). Concomitantly tested flavopiridol yielded 0.8 LCK at its MTD (5.0 mpk, ip, q1d × 8). It was gratifying to see the in vivo efficacy of the CDK2 selective compound **45** in this cyclin E overexpressed model, which is directly related to CDK2 activity. In the human squamous cell carcinoma A431, compound **45** elicited a tumor response of 1 LCK whereas flavopiridol produced only 0.5 LCK at their respective MTDs (24 and 5.0 mpk, ip, q1d × 8). We believe that the efficacy of **45** in vivo stems from its potent CDK2 inhibitory activity, cell activity, and favorable pharmacokinetic profile, particularly its high serum concentration over time (Figure 9).

Conclusion

Metabolically stable oxazole-containing aminothiazole CDK2 inhibitors were discovered and optimized starting from the initial high throughput screening hit **1**. Com-

binatorial and parallel synthesis provided a means of generating a rapid SAR for these inhibitors of CDK2, and many analogues in this series exhibit potent CDK2 inhibitory activity with >10–100-fold selectivity over CDK1 and CDK4 as well as other kinases. The solid state X-ray crystallographic data of these inhibitors bound to the CDK2 protein, combined with modeling studies, provided insight into the binding mode of these inhibitors at the active site of CDK2 and rationale for interpreting the SAR. Many of these analogues displayed potent activity in the 72 h ovarian cancer cell A2780 proliferation assay. Compound **14** exhibited potent cytotoxicity in vitro against a variety of cell lines and reduced the phosphorylation of CDK2 substrates such as RB and histone H1 in in vitro A2780 cells. Cell cycle analysis of **47** at its IC₉₀ concentration in A2780 cells showed a reduction of cell population in S phase and a large increase in the apoptotic fraction. Optimization of the physical properties such as solubility and pharmacokinetics led to compound **45**, which demonstrated good efficacy in vivo in several human cancer cell line xenograft models as well as a murine tumor line driven by cyclin E overexpression. Further studies with this class of compound will be reported in the future.

Experimental Section

All new compounds were homogeneous by thin-layer chromatography (TLC) and reversed-phase high-performance liquid chromatography (HPLC, >99%). Flash chromatography was carried out on E. Merck Kieselgel 60 silica gel (230–400 mesh). All of the reaction solvents used such as tetrahydrofuran (THF), *N,N*-dimethylformamide (DMF), and dichloromethane (CH₂Cl₂) were anhydrous solvents, which were purchased from Aldrich Chemical Co. EDCI and HOBt refer to ethyl dimethylaminopropylcarbodiimide hydrochloride salt and 1-hydroxybenzotriazole, respectively. Preparative HPLC was run on YMC OD S-10 50 mm × 500 mm column eluting with a mixture of solvents A and B (starting from 10% of solvent B to 100% solvent B over 30 min gradient time; solvent A: 10% MeOH/90% H₂O/0.1% TFA; solvent B: 90% MeOH/10% H₂O/0.1% TFA; flow rate, 84 mL/min; UV 254 nm). ¹H NMR and ¹³C NMR spectra were obtained on a JEOL 400 MHz

Table 15. Summary of the Crystallographic Data Collection, Reduction, and Refinement

	5	32	41	41 with cyclin A	46
space group	<i>P2</i> ₁ <i>2</i> ₁ <i>2</i> ₁	<i>P2</i> ₁ <i>2</i> ₁ <i>2</i> ₁	<i>P2</i> ₁ <i>2</i> ₁ <i>2</i> ₁	<i>P6</i> ₂ <i>2</i> <i>2</i>	<i>P2</i> ₁ <i>2</i> ₁ <i>2</i> ₁
<i>a</i> (Å ²)	53.46	53.58	53.22	179.21	53.58
<i>b</i> (Å ²)	71.49	71.62	71.45	179.21	71.62
<i>c</i> (Å ²)	72.05	72.17	72.34	213.29	72.17
max obsvd resolution (Å)	1.8	2.0	2.0	2.6	2.0
highest resolution shell (Å)	1.91–1.8	2.12–2.0	2.12–2.0	2.76–2.6	2.12–2.0
no. of observations	64 507	106 091	49 063	204 401	49 067
no. of unique reflections	21 369	18 817	17 556	52 703	16 965
<i>R</i> _{symm} (on <i>F</i>) (%) ^a	4.9 (18.3)	7.4 (25.3)	7.3 (35.9)	6.1 (36.8)	13.5 (29.3)
mean <i>I</i> / <i>σ</i> (<i>I</i>) ^a	24.5 (4.9)	22.0 (3.4)	12.7 (1.6)	16.2 (2.3)	19.8 (4.5)
completeness (%) ^a	82.4 (40.1)	98.2 (78.8)	82.3 (49.9)	86.5 (71.8)	89.2 (66.6)
<i>R</i> -factor (%) ^a	25.2 (31.3)	25.6 (28.2)	32.0 (44.2)	26.8 (43.0)	27.0 (32.6)
<i>R</i> -free (%) ^a	28.7 (35.0)	29.6 (33.7)	37.8 (46.2)	32.2 (47.0)	32.1 (37.1)
avg <i>B</i> -factor (protein) (Å ²)	27.7	19.9	25.1	41.9	28.2
avg <i>B</i> -factor (ligand) (Å ²)	20.1	32.0	35.4	33.4	21.4
residues in final model	298	298	298	1118	298
total no. of atoms	2537	2496	2483	9203	2480
no. of protein atoms	2397	2397	2397	8994	2397
no. of ligand atoms	18	27	28	56	20
no. of solvent atoms	122	72	58	153	63
rms (bonds) (Å ²)	0.006	0.006	0.008	0.007	0.016
rms (angles) (deg)	1.2	1.2	1.3	1.3	1.96
rms (impropers) (deg)	0.75	0.78	0.88	0.96	1.72

^a Numbers in parentheses represent the values in the highest resolution shell.

CPF-270 spectrometer operating at 270 or 67.5 MHz, respectively, and are reported as parts per million downfield from an internal tetramethylsilane standard. The abbreviations of qn. and sx. in ^1H NMR refer to quintet and sextet, respectively. Melting points are uncorrected.

2-Acetamino-5-thiocyanatothiazole (3). To a mixture of **2** (15.7 g, 100 mmol)¹¹ and pyridine (12 g, 150 mmol) in CH_2Cl_2 (100 mL) was added acetic anhydride (1.2 g, 120 mmol) at room temperature. After it was stirred for 6 h, the mixture was concentrated to dryness and MeOH (50 mL) was added to the residue. The precipitates were collected, washed with water, dried, and recrystallized from MeOH to afford **2** (15.2 g, 76%) as a light yellow solid; mp 212 °C (literature^{11b} 212–214 °C). ^1H NMR (CD_3OD): δ 7.79 (s, 1H), 2.23 (s, 3H).

[[2-(Acetylamino)-5-thiazolyl]thio]acetic Acid 1,1-Dimethylethyl Ester (5). To a mixture of **3** (5.97 g, 30 mmol) in MeOH (360 mL) under argon atmosphere was added DTT (9.26 g, 60 mmol) at room temperature. The mixture was stirred for 2 h and then concentrated in vacuo to afford a solid. The solid was dissolved in DMF (30 mL), and to this solution were added *tert*-butyl bromoacetate (5.85 g, 30 mmol) and potassium carbonate (5.0 g, 36 mmol) at room temperature. The mixture was stirred at room temperature for 2 h, and then, H_2O (200 mL) was added to the reaction mixture. The precipitates were collected, washed with water, dried, dissolved in CH_2Cl_2 (100 mL) and MeOH (10 mL), and filtered through a silica pad. The filtrate was concentrated in vacuo to afford the desired product **5** (7.5 g, 87%) as a light yellow solid; mp 162–163 °C. ^1H NMR (CDCl_3): δ 12.2 (s, 1H), 7.48 (s, 1H), 3.37 (s, 2H), 2.32 (s, 3H), 1.45 (s, 9H). MS (ESI): 289 (M + H)⁺, 287 (M – H)[–]. Anal. ($\text{C}_{11}\text{H}_{16}\text{N}_3\text{O}_3\text{S}_2$) C, H, N, S.

[[2-(Acetylamino)-5-thiazolyl]thio]acetic Acid (6). A solution of ester **5** (4.32 g, 15 mmol) in CH_2Cl_2 (30 mL) and TFA (20 mL) was stirred at room temperature overnight and concentrated. To the residue was added Et_2O (50 mL). The solid was collected, washed with Et_2O , and dried to afford the desired product (3.38 g, 97%) as a solid; mp 210 °C. ^1H NMR (CD_3OD): δ 7.48 (s, 1H), 3.47 (s, 2H), 2.20 (s, 3H). MS (ESI): 231 (M – H)[–]. Anal. ($\text{C}_7\text{H}_8\text{N}_2\text{O}_3\text{S}_2$) C, H, N, S.

[[2-(Acetylamino)-5-thiazolyl]thio]acetic Acid Ethyl Ester (1). It was prepared following the same procedure as in **5** using ethyl bromoacetate instead of *tert*-butyl bromoacetate. ^1H NMR (CDCl_3): δ 7.44 (s, 1H), 4.11 (q, $J = 6.7$ Hz, 2H), 3.40 (s, 2H), 2.27 (s, 3H), 1.20 (t, $J = 6.7$ Hz, 3H). ^{13}C NMR (CDCl_3): δ 168.9, 168.1, 162.8, 141.6, 121.8, 61.8, 40.1, 23.1, 14.1. Anal. ($\text{C}_9\text{H}_{12}\text{N}_2\text{O}_3\text{S}_2$) C, H, N, S.

N-[5-(2-Hydroxy-4,4-dimethyl-pentylsulfanyl)thiazol-2-yl]acetamide (7). To a stirred solution of 5,5-dimethyl-1-hexene (3.45 g, 35.2 mmol) in CH_2Cl_2 (40 mL) at room temperature was added *m*-chloroperoxybenzoic acid (75% purity, 8.49 g, 49.2 mmol). The reaction mixture was stirred at room temperature for 2.5 h. This mixture was washed with 0.1 N NaOH (3 × 30 mL), then diluted with CH_2Cl_2 (15 mL), and washed with 0.1 N NaOH (20 mL) and brine (20 mL). The organic layer was dried (MgSO_4) and filtered to give a solution of 1,2-epoxy-5,5-dimethylhexane in CH_2Cl_2 , which was used in the next reaction directly without any further purification. To a stirred mixture of thioacetate **4** (0.65 g, 3.0 mmol, Applied Chemical Laboratory, Inc.) in EtOH (10 mL) under argon atmosphere at room temperature was added slowly 21% NaOEt solution in EtOH (3.30 mmol). The reaction mixture was purged with argon for 5 min. To this mixture was then added 1,2-epoxy-5,5-dimethylhexane (4.48 mmol) in CH_2Cl_2 (7.0 mL) obtained above. The reaction mixture was again purged with argon for 5 min and stirred at room temperature for 19 h. The reaction mixture was concentrated in vacuo and mixed with saturated NaHCO_3 (100 mL), and the product was extracted with EtOAc (2 × 120 mL) and CH_2Cl_2 (120 mL). The combined organic extracts were washed with 5% KHSO_4 (40 mL), saturated NaHCO_3 (40 mL), and brine (40 mL). The organic layer was dried over MgSO_4 and concentrated in vacuo to give a crude oil, which was purified by flash column chromatography on silica gel eluting with 25% EtOAc in CH_2Cl_2 to obtain **7** (0.20 g, 23%). ^1H NMR (CD_3OD): δ 7.35 (s,

1H), 3.81–3.73 (m, 1H), 2.80–2.67 (m, 2H), 2.29 (s, 3H), 1.53–1.32 (m, 2H), 0.93 (s, 9H). ^{13}C NMR (CD_3OD): δ 169.5, 160.9, 142.8, 123.1, 67.6, 49.9, 47.0, 29.9, 29.4, 21.4. MS (ESI): 288.9 (M + H)⁺, 287.2 (M – H)[–]. Anal. ($\text{C}_{12}\text{H}_{20}\text{N}_2\text{O}_2\text{S}_2$) C, H, N, S.

N-[5-[(4,4-Dimethyl-2-oxopentyl)thio]-2-thiazolyl]acetamide (8). To a stirred solution of alcohol **7** (40.2 mg, 0.14 mmol) in CH_2Cl_2 (1.2 mL) was added Dess–Martin periodinane (211 mg, 0.5 mmol)²² at room temperature and stirred at room temperature overnight. The reaction mixture was diluted with CH_2Cl_2 (120 mL) and washed with 0.1 N NaOH (2 × 30 mL) followed by saturated NaHCO_3 (30 mL) and brine (30 mL). The organic layer was dried over MgSO_4 , filtered, and concentrated in vacuo. The residue was chromatographed on silica gel eluting with 2% CH_3OH in CH_2Cl_2 to give the partially purified product (28.8 mg). This was further purified by a preparative TLC (SiO_2) eluting with 4% CH_3OH in CH_2Cl_2 to obtain desired product **8** as a light yellow solid (13.2 mg, 33%); mp 163–164 °C. ^1H NMR (CDCl_3): δ 7.42 (s, 1H), 3.51 (s, 2H), 2.45 (s, 2H), 2.30 (s, 3H), 1.01 (s, 9H). MS (ESI): 287.12 (M + H)⁺. Anal. ($\text{C}_{12}\text{H}_{18}\text{N}_2\text{O}_2\text{S}_2 \cdot 0.25\text{H}_2\text{O}$) C, H, N, S.

N-[5-[[2-(1,1-Dimethylethoxy)ethyl]thio]-2-thiazolyl]acetamide (9). To a stirred mixture of 2-*tert*-butoxyethanol (3.0 g, 25.3 mmol) and Et_3N (35.5 mmol) in CH_2Cl_2 (40 mL) at 0 °C was added methanesulfonyl chloride (2.4 mL, 30 mmol) slowly. The reaction mixture was stirred at 0 °C for 2 h, diluted with CH_2Cl_2 (160 mL), and then was washed with 1 N HCl solution (3 × 40 mL) followed by saturated NaHCO_3 (2 × 40 mL) and brine (40 mL). The organic layer was dried (MgSO_4), filtered, and concentrated in vacuo to give crude 2-*tert*-butoxyethyl methanesulfonate in a quantitative yield as an oil, which was used for the next step without any further purification.

To a stirred mixture of thioacetate **4** (185 mg, 0.86 mmol) in THF (10 mL) under argon at room temperature was added KO^tBu (0.94 mL of 1 M solution in THF, 0.94 mmol). To this mixture was added methanesulfonyl compound obtained above (250 mg, 1.28 mmol) in THF (1 mL). The reaction mixture was purged with argon for 2 min and heated at 55 °C for 16 h. The mixture was cooled to room temperature, diluted with EtOAc (100 mL), and washed with water (30 mL) followed by saturated NaHCO_3 (2 × 30 mL) and brine (30 mL). The organic layer was dried over MgSO_4 , filtered, and concentrated in vacuo. This was chromatographed on silica gel eluting with 2% CH_3OH in CH_2Cl_2 to obtain **9** as a light yellow solid (120 mg, 51%); mp 119–121 °C. ^1H NMR (CDCl_3): δ 7.35 (s, 1H), 3.50 (t, $J = 6.4$ Hz, 3H), 2.84 (t, $J = 6.4$ Hz, 3H), 2.28 (s, 3H), 1.13 (s, 9H). ^{13}C NMR (CDCl_3): δ 168.1, 162.1, 139.1, 124.4, 73.6, 60.8, 39.0, 27.5, 23.1. MS (ESI): 275.2 (M + H)⁺. Anal. ($\text{C}_{11}\text{H}_{17}\text{N}_2\text{O}_2\text{S}_2$) C, H, N, S.

N-[5-[(2-Phenylethyl)thio]-2-thiazolyl]acetamide (10). A solution of KO^tBu in THF (0.51 mL of 1 M solution, 0.51 mmol) was added to a stirred mixture of **4** (100 mg, 0.46 mmol) in dry THF (5 mL) under argon atmosphere. After it was stirred for 10 min, a solution of phenethyl bromide (103 mg, 0.56 mmol) in THF (1 mL) was added and the mixture was heated at 55 °C for 7 h. It was cooled to room temperature and concentrated in vacuo, and the residue was purified by column chromatography on silica gel eluting with CH_2Cl_2 to obtain **10** (104 mg, 81%) as a light yellow solid; mp 172–173 °C. ^1H NMR (CDCl_3): δ 7.40–7.17 (m, 5H), 3.00 (t, $J = 5.6$ Hz, 2H), 2.91 (t, $J = 5.6$ Hz, 2H), 2.33 (s, 3H). ^{13}C NMR (CDCl_3): δ 168.0, 162.0, 142.0, 139.5, 128.6, 126.6, 123.3, 39.6, 36.0, 23.2. HRMS FAB (M + H)⁺ calcd for $\text{C}_{13}\text{H}_{14}\text{N}_2\text{O}_2\text{S}_2$, 279.0626; found, 279.0628.

2-[[2-(Acetylamino)-5-thiazolyl]thio]-*N*-ethyl-*N*-methylacetamide (11). A mixture of **6** (15.0 mg, 0.065 mmol), HOBT (10.0 mg, 0.065 mmol), and EDCI (25 mg, 0.13 mmol) in DMF (0.5 mL) was stirred at 0 °C for 0.5 h, and then, neat *N*-ethylmethylamine (0.1 mL) was added. The mixture was stirred at 0 °C for 2 h and overnight at room temperature. The product was purified directly by preparative HPLC to obtain **11** after lyophilizing (12 mg, 67%) as a light yellow solid of the mixture of 1:1 ratio of rotamers; mp 138–140 °C. ^1H NMR (CDCl_3): δ (a mixture of 1:1 ratio of rotamers) 7.48 and

7.47 (s, 1H), 3.63 and 3.61 (s, 2H), 3.43 and 3.41 (q, $J = 7.0$ Hz, 2H), 3.00 and 2.93 (s, 3H), 2.28 (s, 3H), 1.20 and 1.14 (t, $J = 7.0$ Hz, 3H). MS (ESI): 274 (M + H)⁺, 272 (M - H)⁻. HRMS FAB (M + H)⁺ calcd for C₁₀H₁₆N₃O₂S₂, 274.0684; found, 274.0692.

[[2-(Acetylamino)-5-thiazolyl]thio]acetic Acid Benzyl Ester (12). A mixture of **6** (34.8 mg, 0.15 mmol), benzyl alcohol (24.3 mg, 0.225 mmol), diethyl azodicarboxylate (32.0 mg, 0.18 mmol), and triphenylphosphine (59.0 mg, 0.225 mmol) in THF (1.5 mL) was stirred at 0 °C for 1 h, warmed to room temperature, and was allowed to stay overnight. The mixture was concentrated in vacuo, and the residue was purified by preparative HPLC. The fraction containing the desired product was collected, concentrated, and lyophilized to afford **12** as a beige-colored solid (36.0 mg, 75%); mp 142 °C. ¹H NMR (CDCl₃): δ 7.39 (s, 1H), 7.26–7.33 (m, 5H), 5.30 (s, 2H), 3.50 (s, 2H), 2.26 (s, 3H). MS (ESI): 323 (M + H)⁺, 321 (M - H)⁻. Anal. (C₁₄H₁₄N₂O₃S₂) C, H, N, S.

[[2-(Acetylamino)-5-thiazolyl]thio]-N-(2-oxobutyl)acetamide (13). (A) **1-[(Benzyloxycarbonyl)amino]-2-butanol.** A mixture of 1-amino-2-butanol (5.5 g, 61.8 mmol), benzyl chloroformate (11.5 g, 67.6 mmol), and sodium carbonate (7.16 g, 67.7 mmol) in water (50 mL) was stirred at 0 °C for 3 h. Water (50 mL) was added to the reaction mixture, the product was extracted with CH₂Cl₂ (3 × 20 mL), dried over Na₂SO₄, and concentrated, and the residue was purified by a flash chromatography on SiO₂ eluting with hexanes:EtOAc/10:1 followed by EtOAc to afford 1-benzyloxycarbonylamino-2-butanol (13.9 g, 100%) as an oil. ¹H NMR (CDCl₃): δ 7.30 (m, 5H), 5.45 (s, 1H), 5.06 (s, 2H), 3.57 (s, 1H), 3.31 (m, 1H), 3.04 (m, 1H), 2.91 (m, 1H), 1.43 (m, 2H), 0.91 (t, $J = 7.6$ Hz, 3 H).

(B) **1-[(Benzyloxycarbonyl)amino]-2-butanone.** To a solution of oxalyl chloride (37 mL of 2 M solution in CH₂Cl₂, 74 mmol) in CH₂Cl₂ (60 mL) at -78 °C under argon was added dimethyl sulfoxide (DMSO, 7.8 g, 100 mmol). The mixture was stirred at -78 °C for 20 min, and to this mixture was added a solution of 1-benzyloxycarbonylamino-2-butanol (13.9 g, 61.8 mmol) in CH₂Cl₂ (40 mL). The mixture was stirred at -78 °C for 1 h, and then, Et₃N (21 mL) was added to the mixture. The mixture was warmed to room temperature and washed with 1 N hydrochloric acid followed by aqueous sodium bicarbonate solution. The organic solution was dried over MgSO₄ and concentrated to afford 1-benzyloxycarbonylamino-2-butanone (11.2 g, 82%) as a solid, which was enough pure for the next reaction. ¹H NMR (CDCl₃): δ 7.32 (m, 5H), 5.50 (s, 1H), 5.06 (s, 2H), 4.07 (s, 2H), 2.43 (q, $J = 7.6$ Hz, 2H), 1.06 (t, $J = 7.6$ Hz, 3H).

(C) **1-Amino-2-butanone.** A solution of 1-benzyloxycarbonylamino-2-butanone (9.30 mg, 42 mmol) in ethanol (50 mL) and 1 N hydrochloric acid solution (46 mL) was stirred under hydrogen gas (1 atm) in the presence of Pd/C (1.5 g, 10%) at room temperature for 4 h. The mixture was filtered, and the filtrate solution was concentrated. The residue was triturated with Et₂O to afford 1-amino-2-butanone (5.29 g, 100%) as a white solid of hydrochloride salt. ¹H NMR (CD₃OD): δ 3.97 (s, 2H), 2.60 (q, $J = 7.6$ Hz, 2H), 1.08 (t, $J = 7.6$ Hz, 3H). ¹³C NMR (CD₃OD): δ 203.2, 46.5, 32.6, 6.06.

(D) **[[2-(Acetylamino)-5-thiazolyl]thio]-N-(2-oxobutyl)acetamide (13).** A mixture of acid **6** (9.0 g, 39 mmol), HOBT (5.94 g, 39 mmol), and EDCI (11.16 g, 58 mmol) in DMF (50 mL) was stirred at 0 °C for 0.5 h. To this mixture was added 1-amino-2-butanone hydrochloride (5.27 g, 42.7 mmol) followed by Et₃N (15 mL, 107.5 mmol). The mixture was stirred at 0 °C for 0.5 h and at room temperature for 1 h. Water (200 mL) was added, and the product was extracted with CH₂Cl₂ containing 10% MeOH (5 × 100 mL). The combined extracts were dried over Na₂SO₄ and concentrated, and the residue was triturated with water to obtain **13** as a solid (10.5 g, 90%); mp 195–196 °C. ¹H NMR (CDCl₃): δ 7.53 (s, 1H), 4.14 (s, 2H), 3.46 (s, 2H), 2.50 (q, $J = 7.6$ Hz, 2H), 2.25 (s, 3H), 1.12 (t, $J = 7.6$ Hz, 3H). MS (ESI): 302 (M + H)⁺.

N-[5-[(5-Ethyl-2-oxazolyl)methyl]thio]-2-thiazolyl]acetamide (14). To a solution of **13** (10.5 g, 34.8 mmol) in acetic

anhydride (100 mL) at room temperature was added concentrated sulfuric acid (10 mL). The mixture was stirred at 55–60 °C for 2 h, sodium acetate (15 g, 180 mmol) was added, and it was concentrated in vacuo. To the residue was added cold water (100 mL), the precipitated solid was collected, washed with water, and dried, and the product was purified by flash chromatography on silica gel (CH₂Cl₂:MeOH/100:5) to afford **14** (4.2 g, 43%) as a light yellow solid; mp 147–148 °C. ¹H NMR (CDCl₃): δ 12.47 (s, 1H), 7.29 (s, 1H), 6.61 (s, 1H), 3.91 (s, 2H), 2.64 (q, $J = 7.6$ Hz, 2H), 2.25 (s, 3H), 1.21 (t, $J = 7.6$ Hz, 3H). ¹³C NMR (CDCl₃): δ 168.1, 163.1, 158.9, 155.3, 143.6, 122.0, 120.9, 34.9, 23.0, 19.1, 11.8. MS (ESI): 284 (M + H)⁺. Anal. (C₁₁H₁₃N₃O₂S₂) C, H, N, S.

2-Chloro-N-[1-(hydroxymethyl)propyl]acetamide (15). To a mixture of 2-amino-1-butanol (5.0 mL, 53 mmol) and Et₃N (15.0 mL, 111 mmol) in CH₂Cl₂ (20 mL) at -70 °C was added chloroacetyl chloride (4.6 mL, 58 mmol) dropwise. The reaction mixture was stirred at -70 °C for 15 min, warmed to room temperature, diluted with EtOAc (50 mL), and quenched with water (50 mL). The organic layer was separated, and the aqueous layer was extracted with EtOAc (3 × 30 mL). The combined organic layers were dried over MgSO₄ and concentrated to afford **15** (8.6 g, 98%) as a brown solid. ¹H NMR (CDCl₃): δ 6.75 (bs, 1H), 4.03 (s, 2H), 3.90 (m, 1H), 3.68 (m, 2H), 2.98 (bs, 1H), 1.60 (m, 2H), 0.97 (t, $J = 7.8$ Hz, 3H).

2-Chloro-N-(1-formylpropyl)acetamide (16). To a solution of oxalyl chloride (14.5 mL of 2 M solution in CH₂Cl₂, 29.0 mmol) in CH₂Cl₂ (30 mL) at -78 °C DMSO (2.75 mL, 38.8 mmol) was added dropwise over 5 min. The reaction mixture was stirred at -78 °C for 10 min, and then, **15** (4.0 g, 24 mmol) in CH₂Cl₂ (20 mL) was added dropwise over 15 min. After the reaction mixture was stirred at -78 °C for 40 min, Et₃N (9.4 mL, 68 mmol) was added dropwise over 5 min and the reaction mixture was allowed to warm to room temperature and stirred for 2 h. The precipitated solid was removed by filtration and washed with EtOAc. The organic phase was washed with 1 N HCl (2 × 100 mL) and saturated NaHCO₃ (10 mL), dried over MgSO₄, concentrated, and purified by flash chromatography on silica gel (CH₂Cl₂:MeOH/100:7) to afford **16** (3.7 g, 95%) as a brown oil. ¹H NMR (CDCl₃): δ 9.60 (s, 1H), 7.16 (broad, 1H), 4.52 (m, 1H), 4.12 (s, 2H), 2.05 (m, 1H), 1.80 (m, 1H), 0.97 (t, $J = 7.8$ Hz, 3H).

2-(Chloromethyl)-4-ethyloxazole (17). To a solution of **16** (3.7 g, 23 mmol) in toluene (10 mL) at room temperature was added POCl₃ (6.3 mL, 68 mmol). The reaction mixture was heated at 90 °C for 1 h under nitrogen. After it was cooled to room temperature, the reaction mixture was poured into ice water (10 mL) and the pH was adjusted to 7 with 5 N NaOH. The organic layer was separated, and the aqueous layer was extracted with CH₂Cl₂ (3 × 20 mL). The combined organic layers were concentrated and distilled (105 °C/760 mm Hg) to afford **17** (1.1 g, 31%) as a colorless liquid. ¹H NMR (CDCl₃): δ 7.30 (s, 1H), 4.50 (s, 2H), 2.50 (q, $J = 7.3$ Hz, 2H), 1.22 (t, $J = 7.3$ Hz, 3H).

N-[5-[[4-Ethyl-2-oxazolyl)methyl]thio]-2-thiazolyl]acetamide (18). To a solution of **4** (10 mg, 0.050 mmol) in THF (5 mL) at room temperature was added KO^tBu (0.05 mL of 1.0 M solution in THF, 0.05 mmol). The reaction mixture was stirred at room temperature for 15 min, and then, **17** (15 mg, 0.10 mmol) was added. After it was stirred for 3 h, saturated NaHCO₃ solution (5 mL) was added. The organic layer was separated, and the aqueous layer was extracted with CH₂Cl₂ (3 × 10 mL). The combined organic layers were concentrated, and the residue was purified by flash chromatography on SiO₂ (MeOH:CH₂Cl₂/1:20) to afford **18** (5 mg, 36%) as a white solid. ¹H NMR (CDCl₃): δ 11.25 (s, 1H), 7.34 (s, 1H), 7.31 (s, 1H), 3.95 (s, 2H), 2.50 (q, $J = 6.7$ Hz, 2H), 2.27 (s, 3H), 1.19 (t, $J = 6.7$ Hz, 3H). MS (ESI): 284 (M + H)⁺. HRMS FAB (M + H)⁺ calcd for C₁₁H₁₃N₃O₂S₂, 284.0528; found, 284.0529.

2-(Bromomethyl)-4,5-dimethyloxazole (19). A mixture of 2,4,5-trimethyloxazole (0.50 mL, 4.3 mmol, Aldrich Chemical Co.), *N*-bromosuccinimide (0.77 g, 4.3 mmol), and benzoyl peroxide (0.21 g, 0.86 mmol) in CCl₄ (4 mL) was heated at 76

°C under nitrogen for 3 h. After it was cooled to room temperature, the solid was removed by filtration, the filtrate was washed with saturated NaHCO₃ (20 mL) and concentrated, and the residue was purified by flash chromatography on SiO₂ (hexanes:EtOAc/4:1) to afford **19** (64 mg, 8% yield) as a yellow oil. ¹H NMR (CDCl₃): δ 4.4 (s, 2H), 2.25 (s, 3H), 2.05 (s, 3H).

N-[5-[[[4,5-Dimethyl-2-oxazolyl)methyl]thio]-2-thiazolyl]-acetamide (20). To a solution of **19** (0.050 g, 0.23 mmol) in THF (10 mL) at room temperature KO^tBu (0.25 mL of 1.0 M solution in THF, 0.25 mmol) was added. After the reaction mixture was stirred at room temperature for 15 min, **19** (0.064 g, 0.34 mmol) was added. The reaction mixture was stirred at room temperature for 3 h. Saturated NaHCO₃ solution (20 mL) was added, the organic layer was separated, and the aqueous layer was extracted with CH₂Cl₂ (3 × 20 mL). The combined organic layers were concentrated, and the residue was purified by flash chromatography on silica gel (MeOH:CH₂Cl₂/1:20) to afford **20** (15 mg, 23%) as a yellow solid. ¹H NMR (CDCl₃): δ 11.78 (s, 1H), 7.38 (s, 1H), 3.90 (s, 2H), 2.30 (s, 3H), 2.22 (s, 3H), 2.05 (s, 3H). MS (ESI): 284 (M + H)⁺. HRMS FAB (M + H)⁺ calcd for C₁₁H₁₃N₃O₂S₂, 284.0528; found, 284.0526.

1-Diazo-3,3-dimethyl-2-butanone (21, R = *t*Bu). To a mixture of 40% aqueous KOH solution (15 mL) and Et₂O (50 mL) at 0 °C was added *N*-methyl-*N*-nitro-*N*-nitrosoguanidine (5 g, 68 mmol) in portions with stirring. The mixture was stirred at 0 °C for 0.5 h. The organic phase was decanted into a dry flask and dried over solid KOH pellets to give diazomethane solution (50 mL, ca. 0.5 M by titrating with acetic acid). To the diazomethane solution obtained above at 0 °C was added a solution of trimethylacetyl chloride (1.23 mL, 10 mmol) in Et₂O (1 mL) dropwise with stirring. The mixture was kept at 0 °C for 16 h. The solution was purged with argon to remove the excess diazomethane, and then, Et₂O was removed under reduced pressure to give crude **21** (1.33 g, 10 mmol, 100%) as a yellow liquid, which was used directly in the next step.

2-(Chloromethyl)-5-*tert*-butyloxazole (22d). To a solution of boron trifluoride etherate (2 mL, 16 mmol) in chloroacetonitrile (20 mL, 320 mmol) at 0 °C was added a solution of 1-diazo-3,3-dimethyl-2-butanone (1.33 g, 10 mmol) in chloroacetonitrile (5 mL, 80 mmol) dropwise. The resulting solution was stirred at 0 °C for 0.5 h, and it was poured onto saturated aqueous sodium bicarbonate solution to neutralize the acid. Product was extracted with CH₂Cl₂ (3 × 50 mL), and the combined extracts were dried, concentrated, and purified by flash chromatography on silica gel eluting with CH₂Cl₂ to give **22d** (1.1 g, 6.4 mmol, 64% from the acid chloride) as a yellow liquid. ¹H NMR (CDCl₃): δ 1.30 (s, 9H), 4.58 (s, 2H), 6.68 (s, 1H). ¹³C NMR (CDCl₃): δ 28.56, 31.54, 36.20, 120.51, 157.69, 162.56. MS (ESI): 174 (M + H)⁺.

N-[5-[[[5-*tert*-Butyl-2-oxazolyl)methyl]thio]-2-thiazolyl]-acetamide (25). To a solution of **4** (50 mg, 0.23 mmol) in THF (10 mL) was added KO^tBu solution (0.25 mL of 1 M solution, 0.25 mmol) at room temperature under argon. The heterogeneous mixture was stirred for 15 min, and then, a solution of **22d** (59 mg, 0.34 mmol) in THF (1 mL) was added. It was stirred at room temperature for 16 h, concentrated, and purified by flash chromatography on silica gel (EtOAc:hexanes/1:1 and then EtOAc) to give **25** (44 mg, 0.14 mmol, 61%) as a white solid; mp 141–142 °C. ¹H NMR (CDCl₃): δ 11.03 (broad s, 1H), 7.31 (s, 1H), 6.59 (s, 1H), 3.95 (s, 2H), 2.27 (s, 3H), 1.27 (s, 9H). ¹³C NMR (CDCl₃): δ 167.94, 162.45, 162.12, 159.04, 144.35, 121.24, 120.36, 35.15, 31.71, 28.83, 23.34. MS (ESI): 312 (M + H)⁺. Anal. (C₁₃H₁₇N₃O₂S₂) C, H, N, S.

N-[5-[[[5-Methyl-2-oxazolyl)methyl]thio]-2-thiazolyl]-acetamide (23). Yield, 57%; mp 159–160 °C. ¹H NMR (CDCl₃): δ 11.72 (s, 1H), 7.34 (s, 1H), 6.63 (s, 1H), 3.95 (s, 2H), 2.31 (s, 3H), 2.30 (s, 3H). ¹³C NMR (CDCl₃): δ 167.93, 162.60, 158.94, 149.79, 143.82, 123.24, 120.93, 34.86, 23.03, 10.94. MS (ESI): 270 (M + H)⁺. Anal. (C₁₀H₁₁N₃O₂S₂·0.4H₂O) C, H, N, S.

N-[5-[[[5-Isopropyl-2-oxazolyl)methyl]thio]-2-thiazolyl]-acetamide (24). Yield, 79%; mp 123–124 °C. ¹H NMR

(CDCl₃): δ 11.55 (s, 1H), 7.32 (s, 1H), 6.61 (s, 1H), 3.96 (s, 2H), 2.94 (hept, *J* = 6.8 Hz, 1H), 2.28 (s, 3H), 1.24 (d, *J* = 6.8 Hz, 6H). ¹³C NMR (CDCl₃): δ 167.86, 162.55, 159.23, 158.83, 143.89, 120.94, 34.91, 26.04, 23.08, 20.64. MS (ESI): 298 (M + H)⁺. HRMS FAB (M + H)⁺ calcd for C₁₂H₁₆N₃O₂S₂, 298.0684; found, 298.0687.

N-[5-[[[5-(Cyclohexylmethyl)-2-oxazolyl)methyl]thio]-2-thiazolyl]acetamide (26). Yield, 55%; mp 151–153 °C. ¹H NMR (CDCl₃): δ 7.24 (s, 1H), 6.62 (s, 1H), 3.96 (s, 2H), 2.48 (d, *J* = 7.0 Hz, 2H), 2.31 (s, 3H), 1.50–1.72 (m, 5H), 1.10–1.30 (m, 4H), 0.85–0.95 (m, 2H). HRMS FAB (M + H)⁺ calcd for C₁₆H₂₁N₃O₂S₂, 352.1154; found, 352.1167.

N-[5-[[[5-Phenyl-2-oxazolyl)methyl]thio]-2-thiazolyl]-acetamide (27). Yield, 49%; mp 193–195 °C. ¹H NMR (CDCl₃): δ 7.53 (s, 1H), 7.51 (s, 1H), 7.18–7.35 (m, 5H), 4.00 (s, 2H), 2.18 (s, 3H). ¹³C NMR (CDCl₃): δ 168.1, 162.9, 159.4, 152.4, 141.1, 129.0, 128.8, 127.5, 124.2, 122.3, 121.3, 34.7, 23.0. HRMS FAB (M + H)⁺ calcd for C₁₅H₁₃N₃O₂S₂, 332.0528; found, 332.0513.

5-[[[5-*tert*-Butyl-2-oxazolyl)methyl]thio]-2-thiazolamine (28). A solution of **25** (5.56 g 17.9 mmol) and sodium hydroxide solution (1 M in water, 36 mL, 36 mmol) in ethanol (46 mL) was heated at reflux temperature under argon for 7 h, additional sodium hydroxide solution (1 M in water, 5 mL, 5 mmol) was added, and the mixture was heated for 2 more hours. It was concentrated, and hydrochloric acid solution (1 M in water, 20 mL, 20 mmol) was added (pH ~13) to the residue. The precipitated solid was filtered, washed with water, and purified by a flash column on silica gel (EtOAc, and then EtOAc:MeOH/95:5) to obtain **28** (3.63 g, 75%) as a yellow solid; mp 118–121 °C. ¹H NMR (CDCl₃): δ 6.99 (s, 1H), 6.59 (s, 1H), 5.01 (s, 2H), 3.89 (s, 2H), 1.27 (s, 9H). ¹³C NMR (CDCl₃): δ 171.78, 162.04, 158.65, 141.99, 120.02, 115.49, 34.60, 31.49, 28.59. MS (ESI): 270 (M + H)⁺. Anal. (C₁₁H₁₅N₃OS₂) C, H, N, S.

N-[5-[[[5-*tert*-Butyl-2-oxazolyl)methyl]thio]-2-thiazolyl]-2-isopropylamide (29). To a solution of aminothiazole **28** (0.97 g, 3.6 mmol) and pyridine (0.37 g, 4.7 mmol) in CH₂Cl₂ was slowly added isobutyryl chloride (0.43 g, 4.0 mmol) at ice bath temperature. The reaction mixture was warmed to room temperature and stirred for 4 h. It was diluted with CH₂Cl₂ and washed with saturated aqueous NaHCO₃, and the organic layer was collected, dried over Na₂SO₄, and concentrated to obtain the solid residue, which was recrystallized from EtOAc/hexane (1:3) to give **29** as a white solid (1.14 g, 93%); mp 182–183 °C. ¹H NMR (CDCl₃): δ 11.76 (br, 1H), 7.29 (s, 1H), 6.59 (s, 1H), 3.96 (s, 2H), 2.67 (m, 1H), 1.28 (d, *J* = 6.6 Hz, 6H), 1.25 (s, 9H). ¹³C NMR (CDCl₃): δ 175.09, 162.97, 161.76, 158.81, 143.68, 120.81, 125.13, 35.25, 34.86, 31.41, 28.53, 19.17. MS (ESI): 340 (M + H)⁺. Anal. (C₁₅H₂₁N₂O₂S₂) C, H, N, S.

N-[5-[[[5-*tert*-Butyl-2-oxazolyl)methyl]thio]-2-thiazolyl]-2-*tert*-butylamide (30). mp 133–134 °C. ¹H NMR (CDCl₃): δ 9.66 (br, 1H), 7.32 (s, 1H), 6.60 (s, 1H), 3.92 (s, 2H), 1.29 (s, 9H), 2.25 (s, 9H). ¹³C NMR (CDCl₃): δ 176.24, 161.90, 161.64, 144.61, 120.85, 120.13, 39.08, 34.90, 31.37, 28.65, 28.51, 27.08. MS (ESI): 354 (M + H)⁺. Anal. (C₁₆H₂₃N₂O₂S₂) C, H, N, S.

N-[5-[[[5-*tert*-Butyl-2-oxazolyl)methyl]thio]-2-thiazolyl]-benzamide (31). Yield, 80%; mp 149–150 °C. ¹H NMR (CD₃-OD): δ 7.99 (d, *J* = 7.5 Hz, 2H), 7.64 (t, *J* = 7.5 Hz, 1H), 7.54 (t, *J* = 7.5 Hz, 2H), 7.40 (s, 1H), 6.68 (s, 1H), 4.02 (s, 2H), 1.25 (s, 9H). MS (ESI): 374 (M + H)⁺. HRMS FAB (M – H)[–] calcd for C₁₈H₁₉N₃O₂S₂, 372.0840; found, 372.0837.

(*αR*)-**N-[5-[[[5-*tert*-Butyl-2-oxazolyl)methyl]thio]-2-thiazolyl]-*α*-methylbenzeneacetamide (32)** and (*αS*)-**N-[5-[[[5-*tert*-Butyl-2-oxazolyl)methyl]thio]-2-thiazolyl]-*α*-methylbenzeneacetamide (33)**. Compounds **32** and **33** were prepared by coupling with (*R*)- and (*S*)-mandelic acid to obtain the products as glassy material in 50 and 53% yields, respectively. Compound **32**: ¹H NMR (CDCl₃): δ 7.29–7.19 (m, 5H), 7.18 (s, 1H), 6.49 (s, 1H), 3.86 (s, 2H), 3.72 (q, *J* = 7.0 Hz, 1H), 1.52 (d, *J* = 7.0 Hz, 3H), 1.15 (s, 9H), NH of amide: too broad to assign. ¹³C NMR (CDCl₃): δ 179.7, 172.1, 162.2, 161.7,

158.7, 143.6, 139.4, 119.1, 127.8, 127.5, 121.0, 120.1, 46.7, 45.7, 34.8, 31.4, 28.5, 18.4. MS (ESI): 402 (M + H)⁺. Anal. (C₂₀H₂₃N₃O₂S₂) C, H, N, S.

[5-[[[5-*tert*-Butyl-2-oxazolyl]methyl]thio]-2-thiazolyl]-isopropyl Carbamate (34). A solution of **28** (162 g, 0.6 mmol), isopropyl chloroformate (1 M in toluene, 0.72 mL, 0.72 mmol), pyridine (0.2 mL, 2.5 mmol), and 4-(dimethylamino)pyridine (26 mg, 0.21 mmol) in CH₂Cl₂ (10 mL) was stirred at room temperature overnight. Water (20 mL) and EtOAc (20 mL) were added to the reaction mixture. The organic solution was separated, and the aqueous layer was washed with EtOAc (30 mL). The combined organic solutions were dried (Na₂SO₄) and concentrated, and the residue was purified by flash chromatography on silica gel (EtOAc:hexanes/1:2, and then EtOAc:hexanes/1:1) to afford **34** (194 mg, 91%) as a white solid; mp 100–101 °C. ¹H NMR (CDCl₃): δ 12.48 (s, 1H), 7.20 (s, 1H), 6.56 (s, 1H), 5.03 (hept, *J* = 6.2 Hz, 1H), 3.91 (s, 2H), 1.31 (d, *J* = 6.2 Hz, 6H), 1.20 (s, 9H). ¹³C NMR (CDCl₃): δ 165.07, 161.54, 158.81, 153.21, 144.29, 120.02, 119.44, 70.14, 34.78, 31.29, 28.43, 21.83. MS (ESI): 356 (M + H)⁺. Anal. (C₁₅H₂₁N₃O₃S₂·0.2H₂O) C, H, N, S.

[5-[[[5-*tert*-Butyl-2-oxazolyl]methyl]thio]-2-thiazolyl]-benzyl Carbamate (35). Yield, 93%; mp 126–127 °C. ¹H NMR (CDCl₃): δ 12.67 (s, 1H), 7.35–7.40 (m, 5H), 7.11 (s, 1H), 6.55 (s, 1H), 5.24 (s, 2H), 3.89 (s, 2H), 1.19 (s, 9H). ¹³C NMR (CDCl₃): δ 164.70, 161.54, 158.81, 153.45, 144.43, 135.21, 128.62, 128.58, 128.25, 120.00, 119.84, 67.94, 34.72, 31.25, 28.41. MS (ESI): 404 (M + H)⁺. Anal. (C₁₉H₂₁N₃O₃S₂) C, H, N, S.

***N*-[5-[[[5-*tert*-Butyl-2-oxazolyl]methyl]thio]-2-thiazolyl]-benzenesulfonamide (36).** To a solution of **28** (162 mg, 0.6 mmol) in pyridine (1 mL) was added benzenesulfonyl chloride (0.9 mmol) under argon with stirring. The reaction mixture was stirred at 50 °C for 2.5 h. Additional benzenesulfonyl chloride (0.9 mmol) was added dropwise with stirring at 50 °C, and the mixture was stirred at 60 °C for 5 h. To the mixture was added EtOAc (50 mL) and washed with water (5 mL), aqueous HCl (1 M solution, 5 mL), and water. The organic solution was separated, dried (Na₂SO₄), concentrated, and purified by a flash chromatography on silica gel (EtOAc:heptane/1:1, and then EtOAc) to afford a yellow solid, which was recrystallized (EtOAc:heptane) to give **36** (143 mg, 58%) as a white solid; mp 189–190 °C. ¹H NMR (DMSO-*d*₆): δ 12.88 (s, 1H), 7.78 (d, *J* = 7.1 Hz, 2H), 7.62 (t, *J* = 7.4 Hz, 1H), 7.56 (t, *J* = 7.4 Hz, 2H), 7.38 (s, 1H), 6.75 (s, 1H), 4.11 (s, 2H), 1.19 (s, 9H). ¹³C NMR (DMSO-*d*₆): δ 169.36, 160.76, 158.05, 141.73, 132.01, 131.36, 128.75, 125.36, 119.84, 112.27, 32.665, 30.68, 28.01. MS (ESI): 410 (M + H)⁺. Anal. (C₁₇H₁₉N₃O₃S₂) C, H, N, S.

***N*-[5-[[[5-*tert*-Butyl-2-oxazolyl]methyl]thio]-2-thiazolyl]-*N*-methyl-2-isopropylamide (37).** To a mixture of **29** (102 mg, 0.30 mmol) and methyl iodide (86 mg, 0.61 mmol) in DMF (2 mL) was added K₂CO₃ (80 mg, 0.58 mmol) at 0 °C. The mixture was stirred at 0 °C and then at room temperature for 7 h. EtOAc (60 mL) and H₂O (40 mL) were added to the reaction mixture. The organic solution was separated, and the aqueous solution was washed with ethyl acetate (50 mL). The combined organic solutions were dried (Na₂SO₄) and concentrated, and the crude product was purified by flash chromatography on silica gel (EtOAc:hexanes/1:2, and then EtOAc:hexanes/1:1) to afford **37** (66 mg, 62%) as a yellow liquid. ¹H NMR (CDCl₃): δ 7.37 (s, 1H), 6.58 (s, 1H), 3.93 (s, 2H), 3.70 (s, 3H), 3.07 (hept, *J* = 6.7 Hz, 1H), 1.26 (d, *J* = 6.7 Hz, 6H), 1.24 (s, 9H). ¹³C NMR (CDCl₃): δ 176.81, 163.42, 161.97, 159.40, 144.81, 121.84, 120.48, 35.29, 34.57, 32.45, 31.78, 28.90, 19.42. MS (ESI): 354 (M + H)⁺. HRMS FAB (M + H)⁺ calcd for C₁₆H₂₄N₃O₂S₂, 354.1310; found, 354.1296.

***N*-[5-[[[5-*tert*-Butyl-2-oxazolyl]methyl]thio]-2-thiazolyl]-*N*-ethylurea (38).** To a solution of **28** (162 mg, 0.6 mmol) in THF (10 mL) was added ethyl isocyanate (0.12 mL, 1.4 mmol) under argon at room temperature, and the mixture was stirred at 55 °C for 68 h. It was concentrated and purified by flash chromatography on silica gel (EtOAc:heptane/1:1, and then EtOAc) to afford **38** (98 mg, 48%) as a yellow glassy material. ¹H NMR (CDCl₃): δ 7.15 (s, 1H), 6.57 (s, 1H), 3.91 (s, 2H),

3.32 (q, *J* = 6.7 Hz, 2H), 1.21 (s, 9H), 1.17 (t, *J* = 6.7 Hz, 3H). ¹³C NMR (CDCl₃): δ 165.57, 161.74, 158.91, 154.33, 144.65, 120.00, 118.35, 34.98, 34.80, 31.37, 28.51, 15.14. MS (ESI): 341 (M + H)⁺. Anal. (C₁₄H₂₀N₄O₂S₂) C, H, N, S.

***N*-[5-[[[5-*tert*-Butyl-2-oxazolyl]methyl]thio]-2-thiazolyl]-*N*-(4-fluorophenyl)urea (39).** Yield, 83%. ¹H NMR (acetone-*d*₆): δ 7.58 (dd, *J*₁ = 4.9 Hz, *J*₂ = 4.2 Hz, 2H), 7.25 (s, 1H), 7.11 (dd, *J*₁ = *J*₂ = 8.8 Hz, 2H), 6.65 (s, 1H), 4.01 (s, 2H), 1.26 (s, 9H). ¹³C NMR (acetone-*d*₆): δ 164.7, 161.9, 160.4, 159.1, 158.0, 151.9, 144.6, 133.3, 121.8, 119.6, 115.6, 115.4, 34.7, 31.3, 28.6. MS (ESI): 407.09 (M + H)⁺. Anal. (C₁₈H₁₉FN₄O₂S₂) C, H, N, S, F.

***N*-(2,6-Difluorophenyl)-*N*-[5-[[[5-*tert*-butyl-2-oxazolyl]-methyl]thio]-2-thiazolyl]urea (40).** To a stirred mixture of aminothiazole **28** (50 mg, 0.19 mmol) in DMF (1.2 mL) was added 2,6-difluorophenylisocyanate (57.8 mg, 0.37 mmol). The mixture was heated at 90 °C for 3.5 h, additional 2,6-difluorophenylisocyanate (15 mg, 0.01 mmol) was added, and the reaction mixture was further heated at 90 °C for 3 h. It was concentrated in vacuo and purified by preparative HPLC to give the desired compound in 51 mg (65%) as a white solid; mp 133–134 °C. ¹H NMR (CD₃OD): δ 7.35–7.60 (m, 1H), 7.24 (s, 1H), 7.06 (t, *J* = 7.9 Hz, 2H), 6.67 (s, 1H), 4.85 (s, 2H), 1.24 (s, 9H). MS (ESI): 425.9 (M + H)⁺, 423.1 (M – H)[–]. Anal. (C₁₈H₁₈F₂N₄O₂S₂) C, H, N, S.

***N*-(2,6-Dichlorophenyl)-*N*-[5-[[[5-*tert*-butyl-2-oxazolyl]-methyl]thio]-2-thiazolyl]urea (41).** Yield, 59%; mp 88–89 °C. ¹H NMR (CDCl₃): δ 7.39 (d, *J* = 8.3 Hz, 2H), 7.23 (t, *J* = 8.3 Hz, 1H), 6.63 (s, 1H), 3.98 (s, 2H), 1.27 (s, 9H). MS (ESI): 458, 459 (M + H)⁺.

4-(Bromomethyl)-*N*-[5-[[[5-*tert*-butyl-2-oxazolyl]methyl]thio]-2-thiazolyl]benzeneacetamide (43). To a stirred mixture of **28** (8.01 g, 29.7 mmol) and EDCI (6.83 g, 35.6 mmol) in CH₂Cl₂ (100 mL) at room temperature under nitrogen was added **42** (10.26 g, 44.8 mmol, Aldrich Chemical Co.). The reaction mixture was stirred at room temperature for 30 min, diluted with EtOAc (300 mL), and washed with H₂O (60 mL), saturated NaHCO₃ solution (2 × 60 mL), and brine (2 × 60 mL). The organic solution was dried over MgSO₄ and concentrated, and the residue solid was triturated with ethyl ether to obtain **43** (11.0 g, 77%). ¹H NMR (CDCl₃): δ 7.39 (d, *J* = 8.36 Hz, 2H), 7.30 (s, 1H), 7.27 (d, *J* = 8.36 Hz, 2H), 6.55 (s, 1H), 4.49 (s, 2H), 3.94 (s, 2H), 3.80 (s, 2H), 1.23 (s, 9H). MS (ESI): 481.98 (M + H)⁺.

***N*-[5-[[[5-*tert*-Butyl-2-oxazolyl]methyl]thio]-2-thiazolyl]-4-[[[bis(hydroxymethyl)methyl]amino]methyl]benzeneacetamide Hydrochloride Salt (45).** To a mixture of serinol **44** (5.0 g, 55 mmol) in THF (20 mL) and DMF (20 mL) at room temperature under nitrogen atmosphere was added **43** (1.5 g, 3.1 mmol) in portions over 10 min, and it was stirred at room temperature overnight. The reaction mixture was diluted with EtOAc (180 mL), washed with 10% citric acid solution and 10% LiCl solution, dried over MgSO₄, and concentrated to a yellow oil, which was purified by flash chromatography on silica gel (15% MeOH in EtOAc with 0.6% NH₄OH) to yield the pure product as a free amine (1.03 g, 62.8%). The free amine was mixed with 1 N HCl (2.1 mL) to give its HCl salt after drying; mp 132–134 °C. ¹H NMR (DMSO-*d*₆): δ 12.56 (s, 1H), 8.89 (s, 1H), 7.50 (d, *J* = 8.14 Hz, 1H), 7.39 (s, 1H), 7.37 (d, *J* = 8.14 Hz, 1H), 6.70 (s, 1H), 4.20 (m, 2H), 4.05 (s, 2H), 3.79 (s, 2H), 3.66 (d, *J* = 2.1 Hz, 4H), 3.05 (q, *J* = 2.1 Hz, 1H). ¹³C NMR (DMSO-*d*₆): δ 169.5, 161.5, 161.1, 159.0, 145.1, 135.5, 130.8, 130.4, 129.6, 120.2, 119.2, 59.6, 57.4, 47.9, 41.4, 34.2, 31.2, 28.5. MS (ESI): 491.3 (M⁺ + H). Anal. (C₂₃H₃₀N₄O₄S₂·HCl) C, H, N, S, Cl.

***N*-[5-[[[5-Ethyl-2-oxazolyl]methyl]thio]-2-thiazolyl]-1-isopropylamide (46).** Yield, 91%; mp 143–144 °C. ¹H NMR (CDCl₃): δ 11.71 (s, 1H), 7.30 (s, 1H), 6.64 (1s, 1H), 3.95 (s, 2H), 2.65 (m, 3H), 1.28 (d, *J* = 7.0 Hz, 6H), 1.23 (t, *J* = 7.6 Hz, 3H). ¹³C NMR (CDCl₃): δ 176.1, 163.9, 159.9, 156.2, 144.8, 123.0, 121.9, 36.3, 35.9, 20.2, 20.1, 12.8. Anal. (C₁₃H₁₇N₃O₂S₂) C, H, N, S.

***N*-[5-[[[5-Ethyl-2-oxazolyl]methyl]thio]-2-thiazolyl]-3-pyridineacetamide (47).** Yield, 49%; mp 166–167 °C. ¹H

NMR (DMSO-*d*₆): δ 8.92 (s, 1H), 8.88 (d, $J = 5.72$ Hz, 1H), 8.55 (d, $J = 7.92$ Hz, 1H), 8.08 (m, 1H), 7.43 (s, 1H), 6.73 (s, 1H), 4.16 (s, 2H), 4.05 (s, 2H), 2.60 (q, $J = 7.48$ Hz, 2H), 1.13 (t, $J = 7.48$ Hz, 1H). ¹³C NMR (DMSO-*d*₆): δ 167.8, 160.6, 158.5, 154.3, 147.3, 144.9, 141.9, 139.8, 134.5, 126.6, 121.6, 119.0, 37.5, 33.8, 18.1, 11.5. MS (ESI): 361.5 (M + H)⁺. Anal. (C₁₆H₁₆N₄O₂S₂·2HCl·0.5H₂O) C, H, N, S, Cl.

[[5-(Acetylamino)-1,3,4-thiadiazol-2-yl]thio]acetic Acid, *tert*-Butyl Ester (48). A mixture of 5-aminothiadiazole-2-mercaptan (1.33 g, 10 mmol, Aldrich Chemical Co.), acetic anhydride (1.1 mL), and pyridine (5 mL) in CH₂Cl₂ (15 mL) was stirred at room temperature for 7 h. To the reaction mixture CHCl₃ (50 mL) and water (100 mL) were added. The precipitated solid was filtered, washed with water, and dried to obtain the thiol (0.62 g) contaminated by its symmetric disulfide. A partially heterogeneous mixture of this mercaptan and disulfide compound in MeOH (30 mL) and DMF (5 mL) was stirred in the presence of DTT (0.62 g) for 1.5 h. Most of the MeOH was removed in vacuo, and K₂CO₃ (0.6 g) was added to the residue in DMF followed by *tert*-butyl bromoacetate (0.9 mL). After it was stirred for 1 h at room temperature, water (100 mL) and CHCl₃ (100 mL) were added to the reaction mixture. The organic solution was separated, dried over MgSO₄, and concentrated, and the remaining solid was triturated with Et₂O to obtain **48** as a yellow solid (0.91 g, 38% overall yield); mp 149–151 °C. ¹H NMR (CDCl₃): δ 3.90 (s, 2H), 2.43 (s, 3H), 1.43 (s, 9H). ¹³C NMR (CDCl₃): δ 168.7, 166.8, 1, 82.9, 36.7, 27.9, 23.0. MS (ESI): 290 (M + H)⁺. Anal. (C₁₀H₁₅N₃O₃S₂) C, H, N, S.

[[5-(Acetylamino)-2-thiazolyl]thio]acetic Acid, Methyl Ester (49). To a stirred mixture of 5-aminothiazole-2-mercaptan (304 mg, 2.29 mmol, Aldrich Chemical Co.) and pyridine (728 mg, 9.20 mmol) in CH₂Cl₂ (4 mL) under argon at 0 °C was added acetyl chloride (0.34 mL, 4.58 mmol). The reaction mixture was purged with argon for 20 min and stirred at room temperature for 17 h. The reaction mixture was diluted with EtOAc (120 mL) and washed with 1 N HCl (2 × 20 mL), saturated NaHCO₃ (20 mL), and brine (20 mL). The organic layer was dried (MgSO₄), filtered, and concentrated in vacuo. The residue was chromatographed on silica gel eluting with 50% EtOAc in hexanes (120 mL), 70% EtOAc in hexanes (100 mL), and 80% EtOAc in hexanes (100 mL) to give desired thioacetate **49** (78.4 mg, 16%) as an oil. ¹H NMR (CDCl₃): δ 6.51 (s, 1H), 2.23 (s, 3H), 2.10 (s, 3H).

***N*-[2-[[[(5-*tert*-Butyl-2-oxazolyl)methyl]thio]-5-thiazolyl]acetamide (50).** To a stirred mixture of thioacetate **49** (78.4 mg, 0.36 mmol) in THF (3 mL) under argon was added KO^{*t*}Bu (0.40 mL of 1 M solution in THF, 0.40 mmol). The resulting mixture was purged with argon and was added to a solution of 2-chloromethyl-4-*tert*-butyl-oxazole **22d** (69.2 mg, 0.40 mmol). After it was stirred at room temperature for 16 h, the reaction mixture was diluted with saturated NH₄Cl (60 mL) solution and extracted with EtOAc (3 × 80 mL). The combined EtOAc extracts were dried (MgSO₄) and concentrated, and the residue was chromatographed on silica gel eluting with 4% CH₃OH in CH₂Cl₂ to give **50** (81.1 mg, 72%) as an oil. ¹H NMR (CDCl₃): δ 7.11 (s, 1H), 6.58 (s, 1H), 4.32 (s, 2H), 2.17 (s, 3H), 1.28 (s, 9H). ¹³C NMR (CDCl₃): δ 167.3, 162.4, 158.9, 151.4, 137.4, 127.7, 119.3, 31.6, 31.4, 28.4, 22.6. MS (ESI): 312.2 (M + H)⁺.

***N*-[5-[[[(5-*tert*-Butyl-2-oxazolyl)methyl]sulfinyl]-2-thiazolyl]-2-isopropylamide (51).** A mixture of compound **29** (20 mg, 0.059 mmol) and *m*-chloroperoxybenzoic acid (75% purity, 20 mg, 0.064 mmol) in CH₂Cl₂ (5 mL) was stirred at room temperature for 2 h. The reaction mixture was diluted with CH₂Cl₂, washed with aqueous NaHCO₃ solution, dried over MgSO₄, and purified by flash column on silica gel (EtOAc/Hexane 4:1 to 9:1) to give **51** as a colorless oil (8 mg, 34%). ¹H NMR (CDCl₃): δ 7.62 (s, 1H), 6.66 (s, 1H), 4.55 (AB q, $J_1 = 28.5$ Hz, $J_2 = 9.5$ Hz, 2H), 2.70 (hept, $J = 6.84$ Hz, 1H), 1.30 (d, $J = 6.84$ Hz, 6H), 1.16 (s, 9H). ¹³C NMR (DMSO): δ 175.7, 164.6, 163.0, 153.0, 140.9, 133.0, 121.3, 56.2, 35.8, 31.8, 28.7, 19.4. MS (ESI): 356.4 (M + H)⁺.

***N*-[5-[[[(5-*tert*-Butyl-2-oxazolyl)methyl]sulfonyl]-2-thiazolyl]-2-isopropylamide (52).** A mixture of compound **29** (50

mg, 0.147 mmol) and *m*-chloroperoxybenzoic acid (100 mg, 0.319 mmol) in CH₂Cl₂ (5 mL) was stirred at room temperature overnight. The reaction mixture was diluted with CH₂Cl₂, washed with aqueous NaHCO₃ solution, dried over MgSO₄, and purified by flash column on silica gel (EtOAc/Hexane 1:3) to give **52** as a white solid (12 mg, 22%); mp 217–218 °C. ¹H NMR (CDCl₃): δ 10.35 (s, 1H), 7.81 (s, 1H), 6.70 (s, 1H), 4.68 (s, 2H), 2.70 (hept, $J = 6.84$ Hz, 1H), 1.31 (d, $J = 6.84$ Hz, 6H), 1.26 (s, 9H). MS (ESI): 372.1 (M + H)⁺. HRMS FAB (M – H)[–] calcd for C₁₅H₂₁N₃O₄S₂, 370.0895; found, 370.0886.

General Procedure for Solid Phase Synthesis of Aminothiazole CDK Kinase Inhibitors: Synthesis of *N*-[5-[[[(5-*tert*-Butyl-2-oxazolyl)methyl]thio]-2-thiazolyl]-*tert*-butylamide (30). *N*-[[5-Thiocyanato)-2-thiazolyl]trifluoroacetamide (55). To a mixture of 5-thiocyanato-2-aminothiazole (4.7 g, 30 mmol) and 2,6-lutidine (3.75 g, 35 mmol) in THF (25 mL) and CH₂Cl₂ (50 mL) at –78 °C under argon was slowly added trifluoroacetic anhydride (6.86 g, 33 mmol). The mixture was allowed to warm to room temperature and stirred overnight, diluted with CH₂Cl₂ (100 mL), and washed with 5% aqueous citric acid, followed by brine. The organic layer was dried (MgSO₄) and passed through a pad of silica gel. The filtrate was concentrated to afford a light brown solid **55** (5.3 g, 70%). ¹H NMR (CDCl₃): δ 12.4 (br, 1H), 7.83 (s, 1H). MS (ESI): 254 (M + H)⁺.

4-(Chloromethyl)-3-methoxyphenoxy Merrifield Resin (54). To a solution of PPh₃ (17 g, 65 mmol) in CH₂Cl₂ (200 mL) at 0 °C was slowly added triphosgene (9.2 g, 31 mmol) portionwise over 30 min. After this was added, the reaction mixture was stirred at 0 °C for 10 min. The solvent was removed in vacuo, the residue was then dissolved in CH₂Cl₂ (200 mL), and here was added SASRIN resin **53** (12 g, 12 mmol). The resulting mixture was agitated for 4 h, and the resin was washed with dry CH₂Cl₂ (6×) and dried in vacuo.

3-Methoxy-4-[[[(5-thiocyanato-2-thiazolyl)(trifluoroacetyl)amino]methyl]phenoxy Merrifield Resin (56). A mixture of resin-bound benzyl chloride **54** (15 g), thiazole **55** (14 g, 55.3 mmol), and diisopropylethylamine (7.8 mL, 45 mmol) in DMF (50 mL) and CH₂Cl₂ (100 mL) was agitated overnight. The resin **56** was washed with DMF (2×), MeOH (2×), and CH₂Cl₂ (4×) and dried in vacuo.

4-[[[(5-Mercapto-2-thiazolyl)(trifluoroacetyl)amino]methyl]-3-methoxyphenoxy Merrifield Resin (57). A mixture of resin-bound thiocyanate **56** (18.5 g) and DTT (12 g, 78 mmol) in THF (100 mL) and MeOH (100 mL) was agitated overnight. The resin **57** was washed with DMF (2×), MeOH (2×), and CH₂Cl₂ (4×), dried in vacuo, and stored under argon at –20 °C.

4-[[[5-[[[(5-*tert*-Butyl-2-oxazolyl)methyl]thio]-2-thiazolyl](trifluoroacetyl)amino]methyl]-3-methoxyphenoxy Merrifield Resin (58). A stream of argon was bubbled through a mixture of resin-bound thiol **57** (500 mg), **22** (2.0 mmol, R = *t*Bu), and DBU (0.23 mL, 1.5 mmol) in DMF (3 mL) for 5 min, and then, it was heated at 80 °C for 2 h. The resin was washed with DMF (2×), MeOH (2×), and CH₂Cl₂ (4×) and dried in vacuo.

4-*N*-[5-[[[(5-*tert*-Butyl-2-oxazolyl)methyl]thio]-2-thiazolyl]methyl-3-methoxyphenoxy Merrifield Resin (59). A mixture of resin-bound trifluoroacetyl amide **58** (500 mg) and sodium borohydride (4 mmol) in THF (2 mL) and ethanol (2 mL) was agitated overnight. The resin **59** was washed with 50% DMF/H₂O (2×), DMF (2×), MeOH (2×), and CH₂Cl₂ (4×) and dried in vacuo.

4-[[[5-[[[(5-*tert*-Butyl-2-oxazolyl)methyl]thio]-2-thiazolyl](2,2-dimethyl-1-oxopropyl)amino]methyl]-3-methoxyphenoxy Merrifield Resin (60). To a mixture of resin-bound amine **59** (100 mg) and diisopropylethylamine (1.2 mmol) in CH₂Cl₂ (2 mL) in a polypropylene tube fitted into an aluminum block that is cooled with circulating 0 °C coolant was added trimethylacetyl chloride (1 mmol). The mixture was agitated at room temperature overnight. The resin was washed with DMF (2×), MeOH (2×), and CH₂Cl₂ (4×) and used in the next step without drying.

N-[5-[(5-*tert*-Butyl-2-oxazolyl)methyl]thio]-2-thiazolyl]-*tert*-butylamide (30). A resin-bound amide **60** (100 mg) was treated with 60% TFA/CH₂Cl₂ (2 mL) in a polypropylene tube fitted with a polyethylene frit and a luer stopcock for 4 h. The solution was drained in a tube and combined with CH₂Cl₂ rinsing of the resin. The solution was concentrated in Speed Vac. The residue was purified by preparative HPLC to afford **30** (11.3 mg) as a white solid; mp 133–134 °C. ¹H NMR (CDCl₃): δ 9.66 (br, 1H), 7.32 (s, 1H), 6.60 (s, 1H), 3.92 (s, 2H), 2.25 (s, 9H), 1.29 (s, 9H). ¹³C NMR (CDCl₃): δ 176.24, 161.90, 161.64, 144.61, 120.85, 120.13, 39.08, 34.90, 31.37, 28.65, 28.51, 27.08. MS (ESI): 354 (M + H)⁺. Anal. (C₁₆H₂₃N₂O₂S₂) C, H, N, S.

Crystal Structure of Human CDK2. Baculovirus insect cells, expressing CDK2 at a level of 100 mg/L of culture, were grown and collected by centrifugation. The CDK2 protein was purified by subjecting the cell lysate to a high-speed ultracentrifuge spin, a fast-flow Q-sepharose column, and an ATP-agarose affinity column. Crystals of CDK2 were grown at room temperature by the hanging drop vapor diffusion method using 35% poly(ethylene glycol) 5000 monomethyl ester, 0.2 M ammonium acetate, 0.1 M *N*-(2-hydroxyethyl)piperazine-*N*-ethanesulfonic acid (HEPES), pH 7.0, as a reservoir solution. The hanging drop consisted of 10 μL of the concentrated protein (13 mg/mL) mixed with an equal volume of reservoir solution. Prior to data collection, crystals were transferred to a vial containing the mother liquor with 2.4–3.0 nM ligand added and allowed to soak for 3 days. For X-ray crystallographic data collection, the crystal was transferred to a vial containing the mother liquor with 15% glycerol added. The crystal was then flash-cooled by transferring the crystal on a nylon loop to a stream of liquid nitrogen at 100 K for data collection. Data were collected on a Siemens Hi-Star area detector system using mirror-focused Cu K radiation from a Rigaku RU-2000 rotating anode. The X-ray intensity data were reduced using program XENGEN and refined by the method of simulated annealing using program XPLOR. The crystallographic data collection, reduction, and refinement are summarized in Table 15.

Crystal Structure of Human CDK2/Cyclin A Complex. Crystals of CDK2 complex with cyclin A and **41** were grown at 4 °C by the hanging drop vapor diffusion method as previously reported.¹⁷ The hanging drop consisted of 10 μL of the concentrated CDK2/Cyclin A complex mixed with an equal volume of reservoir solution containing 21% saturated (NH₄)₂SO₄, 0.5 M KCl, 5 mM DTT, 40 mM HEPES, pH 7.0. For data collection, a crystal, 0.3 mm × 0.15 mm × 0.15 mm, was placed in a cryoprotectant containing 6 M Na Formate in 25 mM HEPES, pH 7.5. The crystal was frozen, and data were collected as described above.

CDK1/Cyclin B1 Kinase Assay. Kinase reactions consisted of 100 ng of baculovirus expressed GST-CDK1/cyclin B1 complex, 1 μg histone H1 (Boehringer Mannheim, Indianapolis, IN), 0.2 μCi ³³P-γ-ATP, 25 μM ATP in 50 μL of kinase buffer (50 mM Tris, pH 8.0, 10 mM MgCl₂, 1 mM EGTA, 0.5 mM DTT). Reactions were incubated for 45 min at 30 °C and stopped by the addition of cold trichloroacetic acid (TCA) to a final concentration of 15%. TCA precipitates were collected onto GF/C unfilter plates (Packard Instrument Co., Meriden, CT) using a Filtermate universal harvester (Packard Instrument Co.), and the filters were quantitated using a TopCount 96 well liquid scintillation counter (Packard Instrument Co.). Dose response curves were generated to determine the concentration required to inhibit 50% of kinase activity (IC₅₀). Compounds were dissolved at 10 mM in DMSO and evaluated at six concentrations, each in triplicate. The final concentration of DMSO in the assay equaled 2%. IC₅₀ values were derived by nonlinear regression analysis and have a coefficient of variance (SD/mean, *n* = 6) = 16%.

CDK2/Cyclin E Kinase Assay. Kinase reactions consisted of 5 ng of baculovirus expressed GST-CDK2/cyclin E complex, 0.5 μg GST-RB fusion protein (amino acids 776–928 of retinoblastoma protein), 0.2 μCi ³³P-γ-ATP, and 25 μM ATP in 50 μL of kinase buffer (50 mM HEPES, pH 8.0, 10 mM MgCl₂, 1 mM EGTA, 2 mM DTT). Reactions were incubated

for 45 min at 30 °C and stopped by the addition of cold TCA to a final concentration of 15%. TCA precipitates were collected onto GF/C unfilter plates (Packard Instrument Co.) using a Filtermate universal harvester (Packard Instrument Co.), and the filters were quantitated using a TopCount 96 well liquid scintillation counter (Packard Instrument Co.). Dose response curves were generated to determine the concentration required inhibiting 50% of kinase activity (IC₅₀). Compounds were dissolved at 10 mM in DMSO and evaluated at six concentrations, each in triplicate. The final concentration of DMSO in the assay equaled 2%. IC₅₀ values were derived by nonlinear regression analysis and have a coefficient of variance (SD/mean, *n* = 6) = 14%.

CDK4/Cyclin D1 Kinase Assay. Kinase reactions consisted of 150 ng of baculovirus expressed GST-CDK4, 280 ng of Stag-cyclin D1, 0.5 μg of GST-RB fusion protein (amino acids 776–928 of retinoblastoma protein), 0.2 μCi ³³P-γ-ATP, and 25 μM ATP in 50 μL of kinase buffer (50 mM HEPES, pH 8.0, 10 mM MgCl₂, 1 mM EGTA, 2 mM DTT). Reactions were incubated for 1 h at 30 °C and stopped by the addition of cold TCA to a final concentration of 15%. TCA precipitates were collected onto GF/C unfilter plates (Packard Instrument Co.) using a Filtermate universal harvester (Packard Instrument Co.), and the filters were quantitated using a TopCount 96 well liquid scintillation counter (Packard Instrument Co.). Dose response curves were generated to determine the concentration required inhibiting 50% of kinase activity (IC₅₀). Compounds were dissolved at 10 mM in DMSO and evaluated at six concentrations, each in triplicate. The final concentration of DMSO in the assay equaled 2%. IC₅₀ values were derived by nonlinear regression analysis and have a coefficient of variance (SD/mean, *n* = 6) = 18%.

HER1/HER2 Kinase Assay. Kinase reactions consisted of 10 ng of baculovirus expressed GST-HER1 or 100 ng of HER2, 100 ng/mL poly(Glu/Tyr) (Sigma), 0.2 μCi ³³P-γ-ATP, and 1 μM ATP in 50 μL of kinase buffer (50 mM Tris, pH 7.5, 10 mM MnCl₂, 0.5 mM DTT). Reactions were incubated for 1 h at 27 °C and stopped by the addition of cold TCA to a final concentration of 15%. TCA precipitates were collected onto GF/C unfilter plates (Packard Instrument Co.) using a Filtermate universal harvester (Packard Instrument Co.), and the filters were quantitated using a TopCount 96 well liquid scintillation counter (Packard Instrument Co.). Dose response curves were generated to determine the concentration required to inhibit 50% of kinase activity (IC₅₀). Compounds were dissolved at 10 mM in dimethyl sulfoxide (DMSO) and evaluated at six concentrations, each in triplicate. The final concentration of DMSO in the assay equaled 1%. IC₅₀ values were derived by nonlinear regression analysis and have a coefficient of variance (SD/mean, *n* = 6) = 16%.

PKC Assays. The procedure is a modification of Amersham's Serine/Threonine kinase SPA assay (Cat. no. RPNQ 0200). The *in vitro* kinase reaction assay is based on the phosphorylation of a serine residue on the biotinylated, PK-Cepsilon specific pseudosubstrate (BES) with the following sequence Biot-ERM₁PRKRQGSVRRRV-OH. The reaction buffer for PKC assays contained 50 mM MOPS (pH 7.2), 1 μM ATP, 5 mM MgCl₂, 1–2 μM BES, 1 μCi/mL of ³³P-γ-ATP, 0.04 mg/mL phosphatidyl serine, and 0.02 mg/mL diacylglycerol. The following enzyme concentrations (ng/mL) were 200 (ε), 400 (δ), 600 (ζ), 200 (α), and 200 (β-1). The PKC α and β-1 assays were supplemented with 10 μM CaCl₂. The reaction was started by the addition of enzyme and the reaction buffer to Optiplates (Packard Instruments) containing the compound. After 30 min at 37 °C, the reaction was stopped by adding 150 μL of stop solution (50 μM ATP, 50 mM ethylenediaminetetraacetic acid (EDTA), 0.1% Triton-X 100, and 2.5 mg/mL streptavidin-coated PVT-SPA beads; Amersham Cat. no. RPNQ0007, in 1 × phosphate-buffered saline (PBS)). The SPA beads were allowed to settle overnight, and the plates were counted in a Packard Topcount.

IKK Assay. Kinase activity was measured with a fluorescence polarization assay using baculovirus-expressed GST-IKK1. Kinase reactions consisted of 40 ng of GST-IKK and

100 μ M GST-IkBa in 20 μ L of buffer containing 5 μ M ATP, 25 mM Tris, pH 7.5, 7.5 mM MgCl₂, 65 μ M DTT, 5% glycerol, and 0.5 mg/mL bovine serum albumin (BSA). Reactions were incubated for 15 min at room temperature before addition of 5.25 nM FITC-IkB peptide and anti-phospho-IkB α (Santa Cruz) in Tris-buffered saline, pH 7.6, containing 100 mM EDTA and 0.1% bovine γ -globulin. After the quenched reaction reached equilibrium, polarized light was measured with an LJL analyst (Molecular Devices Corporation, Sunnyvale, CA).

Emt and ZAP-70 Assays. The protein substrate for the kinase reaction was a glutathione *S*-transferase fusion protein containing the tyrosine kinase phosphorylation sites of the SLP-76 protein (Gst-SLP76). Both Emt and ZAP-70 were generated using a baculovirus expression system. The kinase reactions (60 μ L) containing 25 mM HEPES, pH 7.0, 5 mM MgCl₂, 5 mM MnCl₂, 1 μ M ATP (0.4 μ Ci γ -³³P-ATP), 0.1 mg/mL BSA, 83 μ g/mL Gst-SLP76, 5 ng of enzyme (Emt or ZAP70), and various concentrations of tested compound were carried out at room temperature for 10 min. After it was terminated by adding 100 μ L of 20% TCA and 0.1 mM NaPPi, the precipitated proteins were harvested on a filter plate and washed. The radioactivity incorporated was then determined using a Topcount after adding 30 μ L of Microscint scintillation fluid.

LCK Assay. Kinase reactions were carried out in a 96 well format and consisted of 10 ng of baculovirus-expressed GST-LCK, 5 μ g poly(GLU/Tyr), 0.02 μ Ci of ³³P γ -ATP, 1 μ M ATP in 50 μ L of buffer containing 40 mM HEPES, pH 7.4, 5 mM MnCl₂, 30 μ M DTT, and 0.1 mg/mL BSA. Reactions were incubated for 1 h at 26 °C and stopped by the addition of 2.5 mg/mL BSA in 0.3 M EDTA. The reactions were precipitated on ice with 100 μ L of 3.5 M ATP in 5% TCA. TCA precipitates were collected onto GF/C unfilter plates (Packard Instrument Co.) using a Filtermate universal harvester (Packard Instrument Co.), and the filters were quantitated using a TopCount 96 well liquid scintillation counter (Packard Instrument Co.). Dose response curves were generated to determine the concentration of compounds required to inhibit 50% of kinase activity (IC₅₀). Compounds were dissolved at 10 mM in DMSO and evaluated at six concentrations, each in triplicate. The final concentration of DMSO in the assay equaled 1%. IC₅₀ values were derived by nonlinear regression analysis.

IGF-Receptor Tyrosine Kinase Assay. The IGF-1 receptor tyrosine kinase was assayed using the synthetic polymer poly(Glu/Tyr) (Sigma Chemicals) as a phosphoacceptor substrate. Each reaction mixture consisted of a total volume of 50 μ L and contained 125 ng of baculovirus-expressed enzyme, 2.5 μ g of poly(Glu/Tyr), 25 μ M ATP, and 0.1 μ Ci of [γ -³³P]ATP. The mixtures also contained 20 mM MOPS, pH 7.0, 5 mM MnCl₂, 0.5 mM DDT, and 0.1 mg/mL BSA. The reaction mixtures were incubated at 30 °C for 45 min, and kinase activity was determined by quantification of the amount of radioactive phosphate transferred to the poly(Glu/Tyr) substrate. Addition of cold TCA precipitated the proteins, which were collected onto GF/C unfilter plates (Packard Instrument Co.) using a Filtermate universal harvester, and the filters were quantified using a TopCount 96 well liquid scintillation counter (Packard Instrument Co.). Compounds were dissolved in DMSO to a concentration of 10 mM and were evaluated at six concentrations, each in triplicate. The final concentration of DMSO added to the kinase assays was 0.5%, which has been shown to have no effect on kinase activity. IC₅₀ values were derived from nonlinear regression analysis and have a coefficient of variance (SD/mean, *n* = 6) = 16%.

FAK Tyrosine Kinase Assay. The focal adhesion kinase was assayed using the synthetic polymer poly(Glu/Tyr) (Sigma Chemicals) as a phosphoacceptor substrate. Each reaction mixture consisted of a total volume of 50 μ L and contained 100 ng of baculovirus-expressed enzyme, 2 μ g of poly(Glu/Tyr), 1 μ M ATP, and 0.2 μ Ci of [γ -³³P]ATP. The mixtures also contained 40 mM Tris·HCl, pH 7.4, 1 mM MnCl₂, 0.5 mM DTT, and 0.1 mg/mL BSA. The reaction mixtures were incubated at 26 °C for 1 h, and kinase activity was determined by

quantification of the amount of radioactive phosphate transferred to the poly(Glu/Tyr) substrate. Addition of cold TCA precipitated the proteins, which were collected onto GF/C unfilter plates (Packard Instrument Co.) using a Filtermate universal harvester, and the filters were quantified using a TopCount 96 well liquid scintillation counter (Packard Instrument Co.). Compounds were dissolved in DMSO to a concentration of 10 mM and were evaluated at six concentrations, each in triplicate. The final concentration of DMSO added to the kinase assays was 0.5%, which has been shown to have no effect on kinase activity. IC₅₀ values were derived nonlinear regression analysis and have a coefficient of variance (SD/mean, *n* = 6) = 16%.

Cell Culture. Tissue culture cells were maintained in logarithmic growth in RPMI 1640 medium (Gibco), 5 mM HEPES buffer, and 10% fetal bovine serum (Gibco). Adult bovine aortic endothelial (ABAE) cells (a primary cell line) were grown in RPMI 1640 media containing 2.0 ng/mL basic fibroblast growth factor. The cell line panel is made up of human ovarian carcinoma cell lines (A2780/DDP-S, A2780/DDP-R, A2780/TAX-S, A2780/TAX-R, and OVCAR-3), human breast carcinoma cell lines (MCF-7 and SKBR-3), human prostate carcinoma cell lines (LNCAP and PC-3), human colon carcinoma cell lines (HCT116, HCT116/VM46, HCT116/VP35, Caco-2, LS 174T, and MIP), human lung carcinoma (A549 and LX-1), human squamous cell carcinoma cell line (A431), human leukemia cell lines (CCRF-CEM, HL-60, and K562), human fibroblast cell line (HS27), ABAE, mouse lung carcinoma cell line (M109), and mouse lung fibroblast (p53^{-/-}) cell line (MLF) isolated from p53 knockout mice. The HCT116/VM46 cell line is a multidrug resistant variant of the parental HCT116 cells and overexpresses P-glycoprotein.²³ The HCT116/VP35 cell line is a variant that has low topoisomerase II levels and is resistant to VP-16.²³ The A2780/DDP-R cell line is resistant to cisplatin relative to the parental A2780/DDP-S cells. A tubulin mutation is present in the A2780/TAX-R, which are resistant to paclitaxel relative to the parental A2780/TAX-S cells (provided by Dr. Tito Fojo; NCI, Bethesda, MD).²⁴

72 h Proliferation Assay. In vitro cytotoxicity was assessed in tissue culture cells by MTS (3-(4,5-dimethylthiazol-2-yl)-5-(3-carboxymethoxyphenyl)-2-(4-sulfenyl)-2H-tetrazolium, inner salt) assay as previously described.²³ Depending upon the cell line used, cells were plated at a density of 3000–6000 cells/well, in a 96 well plate, and 24 h later, drugs were added and serial-diluted. The cells were incubated at 37 °C for 72 h at which time the tetrazolium dye, MTS in combination with phenazine methosulfate, was added. After 3 h, the absorbency was measured at 492 nm, which is proportional to the number of viable cells. The results are expressed as IC₅₀ values.

Cell Cycle. Log phase A2780 cells were plated overnight in six well plates before treatment with various concentrations of compounds and harvested by trypsinization. The cells were prepared for flow cytometry according to the Apo-Direct protocol (Pharmingen). Briefly, the cells were fixed in paraformaldehyde and ethanol, washed, resuspended in staining solution of TdT enzyme and FITC-dUTP, washed, and then stained with PI following RNase treatment.

Phosphoprotein Analysis. A2780 cells were exposed to ³²P-orthophosphate (1 mCi/mL of normal growth media plus dialyzed fetal bovine serum) for 4 h in the presence or absence of 3 μ M compound **14**. Treated A2780S cells were harvested at approximately 70% confluence, and total protein was prepared by lysing the cells in RIPA [50 mM Tris (pH 8), 150 mM NaCl, 1% NP-40, 0.5% Na-deoxycolate, 0.1% sodium dodecyl sulfate (SDS), 0.1% Na₃VO₄, 0.1 mM NaF, 10 mM β -glycerophosphate, plus complete protease inhibitors (Boehringer Mannheim)] buffer. Cell pellets were resuspended at a density of <2 \times 10⁷ cells/mL and incubated for 20 min on ice followed by a high speed 14 000 rpm centrifugation. The protein supernatant was then removed from the debris, and protein content was quantitated using the Micro-BCA assay (Pierce). Treated extracts (250 μ g of total protein/immunoprecipitation) were then immunoprecipitated at 4 °C for 1 h using

5 μg of RB, histone H1, or DNA polymerase α specific antibodies and 20 μL of Protein A-sepharose (Pharmacia). Antibodies used were as follows: anti-Rb clone PMG3-245 (BD-Pharmingen, San Diego, CA), anti-DNA pol- α mixture of clones SJK-132-20, SJK-287-38, SJK-237-71, and SDK-043 (STK1). The immunoprecipitated complexes were then washed three times with cold PBS and separated on a 8 or 10% SDS-polyacrylamide gel for RB or DNA polymerase α and histone H1, respectively. The gels were then dried and analyzed by autoradiography.

Pharmacokinetics in Mouse. The pharmacokinetics of flavopiridol, **45**, and **47** were investigated in male Balb-C mice fasted overnight, following a single dose given intraperitoneally (ip). The vehicle used was cremophor:ethanol:water (1:1:8). A total of 15 mice were dosed per compound. Serum samples were collected from each mouse by cardiac puncture. Serum levels were monitored for 6 h after ip dosing. Samples were collected at 0.5, 1, 2, 4, and 6 h after dosing. The mean body weight of the mice was approximately 20 g.

In a second study, the pharmacokinetics of **45** were investigated in male Balb-C mice fasted overnight, following a single dose of 10 mg/kg given either intravenously (IV) or orally by gavage. The vehicle used was ethanol:water (1:9) for both routes of administration. The mice were fed 4 h postdose. A total of 18 mice were dosed; nine by the intravenous route and nine by the oral route. Three serum samples were collected from each mouse, the first two samples by retroorbital bleed (100 μL) and the third sample by cardiac puncture. Serum levels were monitored for 10 h after dosing. Samples were collected at 5, 10, and 30 min, 1, 2, 4, 6, 8, and 10 h after IV dosing and at 10, 20, and 40 min, 1, 2, 4, 6, 8, and 10 h after oral dosing. The mean body weight of the mice was approximately 20 g.

Blood samples collected were allowed to clot on ice and then centrifuged, and the serum was harvested. Samples were stored at $-20\text{ }^{\circ}\text{C}$ until analysis. Samples were analyzed by LC/MS/MS. Composite serum concentration-time profiles were constructed for pharmacokinetic analysis. The pharmacokinetic parameters were derived by noncompartmental methods using the KINETICA software program. The C_{max} and T_{max} values were recorded directly from experimental observations. The AUC_{tot} values were calculated using a combination of linear and log trapezoidal rules. The total body clearance (Cl), MRT, and the steady state volume of distribution (V_{ss}) were also calculated after IV administration. The oral bioavailability (expressed as %) was estimated by taking the ratio of dose-normalized AUC values after oral doses to those after IV doses.

Metabolic Stability. The compound was incubated with mouse and human liver microsomes. The mouse microsomes were prepared by standard methods and were pooled from livers obtained from a group of animals of the same species ($n = 30$). The human microsomes were purchased from In Vitro Technologies (Baltimore, MD) and were pooled from 10 individual donors. The rates of oxidative metabolism were measured under the following conditions: compound, 10 μM final concentration; final microsomal protein concentration approximately 1 mg/mL; NADPH, 1 mM; pH 7.4 potassium phosphate buffer, 56 mM. Incubations were performed at 37 $^{\circ}\text{C}$ and were initiated by the addition of the substrate. Incubations were quenched by the addition of one volume of acetonitrile after 10 min. Samples were analyzed for the parent compound. The percent metabolized was calculated based on the disappearance of the parent compound.

Protein Binding. The extent of protein binding was determined in mouse and human sera. The method involved equilibrium dialysis using 0.134 M phosphate buffer (pH 7.4) and dialysis membranes (Spectrum, Laguna Hills, CA) with a 12 000–14 000 Da molecular mass cutoff. The dialysis cells (Spectrum) were rotated at 20 rpm in a water bath maintained at 37 $^{\circ}\text{C}$. The extent of binding to serum proteins was determined at a nominal concentration of 20 μM ($n = 3$). Aliquots of buffer and serum were taken at 4 h after incubation

and analyzed for the compound. Percent protein bound was calculated from measured concentrations in buffer and serum.

In Vivo Antitumor Testing. Drug Administration. All CDK inhibitors were first dissolved in a mixture of Cremophor/ethanol (50:50) and stored at 4 $^{\circ}\text{C}$; final dilution to the required dosage strength was made with water so that the dosing solutions contained Cremophor/ethanol/water at a ratio of 10:10:80, respectively. Olivomycin was dissolved in saline. The volume of all compounds injected was 0.01 mL/g of mouse weight.

Animals. All rodents were obtained from Harlan Sprague Dawley Co. (Indianapolis, IN) and maintained in an ammonia-free environment in a defined and pathogen-free colony. The animal care program of Bristol-Myers Squibb Pharmaceutical Research Institute is fully accredited by the American Association for Accreditation of Laboratory Animal Care (AAA-LAC).

Murine P388 Leukemia. Female Balb/c \times DBA/2J F1 mice, weighing within a 3 g range, were used in these studies. On day 0, mice were inoculated ip with 10^6 P388 ascites leukemic cells. Mice were randomized into treatment groups and sufficient groups for a bioassay titration of 10^6 to 10^4 cells per mouse. On day 1 postinoculation, mice were given ip injections of CDK inhibitor on a treatment schedule of every day for 7 days (qd \times 7). A positive reference (olivomycin) was included in each study. All drugs were administered in uniform volumes of 0.01 mL/g of mouse weight. The effectiveness of treatment was assessed by comparison of the median postinoculation life span of each group of treated mice (T) with that of controls (C). The ratio of T to C expressed in percentage value (i.e., %T/C) provides quantitative indication of efficacy. A %T/C of 127 or greater is considered an active result.

Solid Tumor Xenografts in Nude Mice. The following tumors were used, A2780 human ovarian carcinoma, Br-cycE murine breast carcinoma, and A431 human squamous cell carcinoma. All solid tumors were maintained in Balb/c nu/nu nude mice. Tumors were propagated as subcutaneous transplants using tumor fragments obtained from donor mice. All tumor implants for efficacy testing were subcutaneous (sc). The required number of animals needed to detect a meaningful response were grouped at the start of the experiment, and each was given a sc implant of a tumor fragment (~ 50 mg) with a 13 gauge trocar. For treatment of early-stage tumors, the animals were again grouped before distribution to the various treatment and control groups. For treatment of animals with advanced-stage disease, tumors were allowed to grow to the predetermined size window (~ 100 mg size, animals with tumors outside the range were excluded) and animals were evenly distributed to various treatment and control groups. Treatment of each animal was based on individual body weight. Treated animals were checked daily for treatment related toxicity/mortality. Each group of animals was weighed before the initiation of treatment (Wt1) and then again following the last treatment dose (Wt2). The difference in body weight (Wt2 – Wt1) provides a measure of treatment-related toxicity. Tumor response was determined by measurement of tumors with a caliper twice a week, until the tumors reach a predetermined "target" size of 1 g. Tumor weights (mg) were estimated from the formula: tumor weight = (length \times width²)/2.

Establishment of Br-CycE Cyclin E Overexpressing Murine Mammary Carcinoma Xenograft and Cell Line. Each nude mouse was given a subcutaneous implant of a tumor fragment (≈ 20 mg) obtained from a donor transgenic cycE mouse bearing a spontaneously arising mammary tumor. Implantation was accomplished using a 13 gauge trocar inserted sc into the dorsal side of the mouse, near the mammary gland. Nude mice were obtained from Harlan Sprague Dawley Co. and maintained in an ammonia-free environment in a defined and pathogen-free colony. Tumor growth was determined by measurement of tumors with a caliper 1–2 times a week, until the tumors reached a prede-

terminated target size of 1 g. Tumor weights (mg) were estimated from the formula: tumor weight = (length × width²)/2. Xenograft cycE tumors grown in nude mice were excised and minced with scissors and were dissociated using an enzyme cocktail consisting of 0.025% collagenase (Sigma Chemical Co.), 0.05% Pronase (Calbiochem, LaJolla, CA), and 0.04% DNase (Sigma) for 1 h at 37 °C. After debris was removed by passing the cell suspensions through 70 μm nylon screens, the cells were washed in PBS, counted, and resuspended in complete RPMI 1640 media supplemented with 10% heat-inactivated fetal bovine serum (GIBCO). Cells (3 × 10E+5) were then seeded onto a variety of Biocoat Cellware (Becton Dickinson) coated separately with the following extracellular matrix: collagen I, laminin, fibronectin, collagen IV, poly-D-lysine.

Acknowledgment. Microanalysis and mass spectra were kindly provided by the Bristol-Myers Squibb Department of Analysis Research and Development.

Note Added after ASAP Posting. This article was released ASAP on 8/2/2002 with a minor error in Table 9. The correct version was posted on 8/22/2002.

References

- (1) (a) Hunter, T.; Pines, J. Cyclins and Cancer II. Cyclin and CDK inhibitors come of age. *Cell* **1994**, *79*, 573–582. (b) Sherr, C. Cancer cell cycles. *Science* **1996**, *274*, 1672–1677.
- (2) A review article: Pines, J. The cell cycle kinases. *Semin. Cancer Biol.* **1994**, *5*, 305–313.
- (3) (a) Kamb, A.; Gruis, N. A.; Weaver-Feldhaus, J.; Liu, Q.; Harshman, K.; Tavtigian, S. V.; Stockert, E.; Day, R. S., III; Johnson, B. E.; Skolnik, M. H. A Cell Cycle Regulators, Potentially Involved in Genesis of Many Tumor Types. *Science* **1994**, *264*, 436–440. (b) Nobori, T.; Miura, K.; Wu, D. J.; Lois, A.; Takabayashi, K.; Carson, D. A. Deletions of the cyclin-dependent kinase-4 inhibitor gene in multiple human cancers. *Nature (London)* **1994**, *368*, 753–756. (c) Pines, J. Cyclins, CDKs and cancer. *Semin. Cancer Biol.* **1995**, *6*, 63–72. (d) Hartwell, L. H.; Kastan, M. B. Cell cycle control and cancer. *Science* **1994**, *266*, 1821–1828.
- (4) (a) Paulovich, A. G.; Toczyski, D. P.; Hartwell, L. H. When checkpoint fails. *Cell* **1997**, *88*, 315–321. (b) Pardee, A. B. A restriction point for control of normal animal cell proliferation. *Proc. Natl. Acad. Sci. U.S.A.* **1974**, *71*, 1286–1290.
- (5) Donnellan, R.; Chetty, R. Cyclin E in human cancers. *FASEB J.* **1999**, *13*, 773–780.
- (6) (a) Catzavelos, C.; Bhattacharya, N.; Ung, Y. C.; Wilson, J. A.; Roncari, L.; Sandhu, C.; Shaw, P.; Yeager, H.; Morava-Protzner, I.; Kapusta, L.; Franssen, E.; Pritchard, K. I.; Slingerland, J. M. Decreased levels of the cell-cycle inhibitor p27^{Kip1} protein: prognostic implications in primary breast cancer. *Nat. Med.* **1997**, *3*, 227–230. (b) Quintanilla-Martinez, L.; Thieblemont, C.; Fend, F.; Kumar, S.; Pinyol, M.; Campo, E.; Jaffe, E. S.; Raffeld, M. Mantle cell lymphomas lack expression of p27^{Kip1}, a cyclin-dependent kinase inhibitor. *Am. J. Pathol.* **1998**, *153*, 175–182. (c) Cordon-Cardo, C.; Koff, A.; Drobnjak, M.; Capodiceci, P.; Osman, I.; Millard, S. S.; Gaudin, M. F.; Zhang, Z.; Massague, J.; Scher, H. I. Distinct altered patterns of p27^{Kip1} gene expression in benign prostatic hyperplasia and prostatic carcinoma. *J. Int. Cancer Inst.* **1998**, *90*, 1284–1291.
- (7) (a) Cote, R. J.; Shi, Y.; Groshen, S.; Feng, A.; Carlos, C.; Skinner, D.; Lieskovosky, G. Association of p27^{Kip1} levels with recurrence and survival in patients with staged C prostate carcinoma. *J. Natl. Cancer Inst.* **1998**, *90*, 916–920. (b) Flrenes, V. A.; Maelandsmo, G. M.; Kerbel, R. S.; Slingerland, J. M.; Nesland, J. M.; Holm, R. Protein expression of the cell-cycle inhibitor p27^{Kip1} in malignant melanoma: inverse correlation with disease-free survival. *Am. J. Pathol.* **1998**, *153*, 305–312.
- (8) (a) Kaur, G.; Stetler-Stevenson, M.; Sebers, S.; Worland, P.; Sedlacek, H.; Myers, C.; Czech, J.; Naik, R.; Sausville, E. Growth Inhibition with Reversible Cell Cycle Arrest of Carcinoma Cells by Flavone L86-8275. *J. Natl. Cancer Inst.* **1992**, *84*, 1736–1740. (b) Kitagawa, M.; Okabe, T.; Ogino, H.; Matsumoto, H.; Suzuki-Takahashi, I.; Kokubo, T.; Higashi, H.; Saitoh, S.; Taya, Y.; Yasuda, H.; Ohba, Y.; Nishimura, S.; Tanaka, N.; Okuyama, A. Butyrolactone I, a selective inhibitor of cdk2 and cdc2 kinase. *Oncogene* **1993**, *8*, 2425–2432. (c) Vesely, J.; Havlicek, L.; Strnad, M.; Blow, J.; Donella-Deana, A.; Pinna, L.; Letham, D. S.; Kato, J.; Detivaud, L.; Leclerc, S.; Meijer, L. Inhibition of cyclin-dependent kinases by purine analogues. *Eur. J. Biochem.* **1994**, *224*, 771–786. (d) Buquet-Fagot, C.; Lallemand, F.; Montagne, M.-N.; Mester, J. Effects of olomucine, a selective inhibitor of cyclin-dependent kinases, on cell cycle progression in human cancer cell lines. *Anti-Cancer Drugs* **1997**, *8*, 623–631. (e) Barvian, M.; Boschelli, D. H.; Cossrow, J.; Dobrusin, E.; Fattaey, A.; Fritsch, A.; Fry, D.; Harvey, P.; Keller, P.; Garrett, M.; La, F.; Leopold, W.; McNamara, D.; Quin, M.; Trumpp-Kallmeyer, S.; Toogood, P.; Wu, Z.; Zhang, E. Pyrido[2,3-d]pyrimidin-7-one inhibitors of cyclin-dependent kinases. *J. Med. Chem.* **2000**, *43*, 4606–4616. (f) Gussio, R.; Zaharevitz, D. W.; McGrath, C. F.; Pattabiraman, N.; Kellogg, G. E.; et al. Structure-based design modifications of the paullone molecular scaffold for cyclin-dependent kinase inhibition. *Anti-Cancer Drug Des.* **2000**, *15*, 53–66. (g) Gray, N. S.; Wodicka, L.; Thunnissen, A.-M. W. H.; Norman, T. C.; Kwon, S.; Espinoza, S. F. H.; Morgan, D. O.; Barnes, G.; LeClerc, S.; Meijer, L.; Kim, S.; Lockhart, D. J.; Schultz, P. G. Exploiting chemical libraries, structure, and genomics in the search for kinase inhibitors. *Science* **1998**, *281*, 533–538. (h) Brooks, E. E.; Gray, N. S.; Joly, A.; Kerwar, S. S.; Lum, R.; Mackman, R. L.; Norman, T.; Rosete, J.; Rowe, M.; Schow, S. R.; Schultz, P. G.; Wang, X.; Wick, M. M.; Shiffman, D. CVT-313, a specific and potent inhibitor of CDK2 that prevents neointimal proliferation. *J. Biol. Chem.* **1997**, *272*, 29207–29211. (i) Legraverand, M.; Ludwig, O.; Bisagni, E.; Leclerc, S.; Meijer, L. Synthesis of C2 alkynylated purines, a new family of potent inhibitors of cyclin-dependent kinases. *Bioorg. Med. Chem. Lett.* **1998**, *8*, 793–798. (j) Kim, K. S.; Sack, J. S.; Tokarski, J. S.; Qian, L.; Chao, S. T.; Leith, L.; Kelly, Y. F.; Misra, R. N.; Hunt, J. T.; Kimball, S. D.; Humphreys, W. G.; Wautlet, B. S.; Janet, G.; Mulheron, J. G.; Webster, K. R. Thio- and Oxoflavopiridols, cyclin-dependent kinase 1 selective inhibitors: synthesis and biological effects. *J. Med. Chem.* **2000**, *43*, 4126–4134. (k) Bramson, H. N.; Corona, J.; Davis, S. T.; Dickerson, S. H.; Edelstein, M.; Frye, S. V.; Gampe, R. T.; Harris, P. A.; Hassell, A.; Holmes, W. D.; Hunter, R. N.; Lackey, K. E.; Lovejoy, B.; Luzzio, M. J.; Montana, V.; Rocque, W. J.; Rusnak, D.; Shewchuk, L.; Veal, J. M.; Walker, D. H.; Kuyper, L. F. Oxindole-based inhibitors of cyclin-dependent kinase 2 (CDK2): Design, synthesis, enzymatic activities, and X-ray crystallographic analysis. *J. Med. Chem.* **2001**, *44*, 4339–4358. (l) Honma, T.; Hayashi, K.; Aoyama, T.; Hashimoto, N.; Machida, T.; Fukasawa, K.; Iwama, T.; Ikeura, C.; Ikuta, M.; Suzuki-Takahashi, I.; Iwasawa, Y.; Hayama, T.; Nishimura, S.; Morishima, H. Structure-Based Generation of a New Class of Potent cdk4 Inhibitors: New de Novo Design Strategy and Library Design. *J. Med. Chem.* **2001**, *44*, 4615–4627. (m) Honma, T.; Yoshizumi, T.; Hashimoto, N.; Hayashi, K.; Kawanishi, N.; Fukasawa, K.; Takaki, T.; Ikeura, C.; Ikuta, M.; Suzuki-Takahashi, I.; Iwasawa, Y.; Hayama, T.; Nishimura, S.; Morishima, H. A Novel Approach for the Development of Selective CDK4 Inhibitors: Library Design Based on Locations of CDK4 Specific Amino Acid Residues. *J. Med. Chem.* **2001**, *44*, 4628–4640. (n) Chong, W. K. M.; Chu, S. S.; Li, L.; Xiao, W.; Yang, Y. 4-Aminothiazole derivatives, their preparation and their use as inhibitors of cyclin-dependent kinases. WO 09921845, May 6, 1999.
- (9) For the review articles, see (a) Webster, K. R. The therapeutic potential of targeting the cell cycle. *Exp. Opin. Invest. Drugs* **1998**, *7* (6), 1–23. (b) Rosania, G. R.; Chang, Y.-T. Targeting hyperproliferative disorders with cyclin dependent kinase inhibitors. *Exp. Opin. Ther. Pat.* **2000**, *10*, 215–230. (c) Sielecki, T. M.; Boylan, J. F.; Benfield, P. A.; Trainor, G. L. Cyclin-Dependent Kinase Inhibitors: Useful Targets in Cell Cycle Regulation. *J. Med. Chem.* **2000**, *43*, 1–18. (d) Gray, N.; Detivaud, L.; Doerig, C.; Meijer, L. ATP-site directed inhibitors of cyclin-dependent kinases. *Curr. Med. Chem.* **1999**, *6*, 859–875. (e) Noble, M. E. M.; Endicott, J. A. Chemical inhibitors of cyclin-dependent kinases: insights into design from X-ray crystallographic studies. *Pharmacol. Ther.* **1999**, *82*, 269–278. (f) Adams, J. L.; Lee, D. Recent progress towards the identification of selective inhibitors of serine/threonine kinases. *Curr. Opin. Drug Discovery Dev.* **1999**, *2*, 96–109.
- (10) Chen, Y.-N. P.; Sharma, S. K.; Ramsey, T. M.; Jiang, L.; Martin, M. S.; Baker, K.; Adams, P. D.; Bair, K. W.; Kaelin, W. G., Jr. Selective killing of transformed cells by cyclin/cyclin-dependent kinase 2 antagonists. *Proc. Natl. Acad. Sci. U.S.A.* **1999**, *96*, 4325–4329.
- (11) (a) Senderowicz, A. M.; Headlee, D.; Stinson, S. F.; Lush, R. M.; Kalil, N.; Villalba, L.; Hill, K.; Steinberg, S. M.; Figg, W. D.; Tompkins, A.; Arbuck, S. G.; Sausville, E. A. Phase I trial of continuous infusion flavopiridol, a novel cyclin-dependent kinase inhibitor, in patients with refractory neoplasms. *J. Clin. Oncol.* **1998**, *16*, 2986–2999. (b) Sedlacek, H. H.; Czech, J.; Naik, R.; Kaur, G.; Worland, P.; Losiewicz, M.; Parker, B.; Carlson, B.; Smith, A.; Senderowicz, A.; Sausville, E. A. Flavopiridol (L868275; NSC 649890), a new kinase inhibitor for tumor therapy. *Int. J. Oncol.* **1996**, *9*, 1143–1168.

- (12) (a) Spadafora, V. J.; Motoyoshi, M. Method and composition for the control of soilborne fungi and prevention of disease caused by them. EP 0625307 A1, 1994, April 22. (b) Hurd, C. D.; Wehrmeister, H. L. The 2-Aminothiazoles. *J. Am. Chem. Soc.* **1949**, *71*, 4007–4010.
- (13) (a) Ibata, T.; Sato, R. The BF_3 catalyzed decomposition of diazocarbonyl compounds in nitriles: synthesis of oxazoles. *Chem. Lett.* **1978**, 1129–1130. (b) Ibata, T.; Isogami, Y. Formation and reaction of oxazoles. Synthesis of N-substituted 2-(aminomethyl)oxazoles. *Bull. Chem. Soc. Jpn.* **1989**, *62*, 618–620.
- (14) Leysen, D. C.; Haemers, A.; Bollaert, W. Thiazolopyridine Analogues of Nalidixic Acid 1. Thiazolo[5,4-b]pyridines. *J. Heterocycl. Chem.* **1984**, *21* (2), 401–406.
- (15) Mergler, M.; Tanner, R.; Grogg, G. P. Peptide synthesis by a combination of solid-phase and solution methods I: a new very acid-labile anchor group for the solid phase synthesis of fully protected fragments. *Tetrahedron Lett.* **1988**, *29*, 4005–4008.
- (16) Rivero, I. A.; Somanathan, R.; Hellberg, L. H. Triphosgene/triphenylphosphine: A mild reagent for the conversion of alcohols to chlorides. *Synth. Commun.* **1993**, *23*, 711–714.
- (17) Brown, P.; Best, D. J.; Broom, N. J. P.; Cassela, R.; O'Hanlon, P. J.; Mitchell, T. J.; Osborne, N. F.; Wilson, J. M. The Chemistry of Pseudomonic Acid. 18. Heterocyclic Replacement of the α,β -Unsaturated Esters: Synthesis, Molecular Modeling, and Antibacterial Activity. *J. Med. Chem.* **1997**, *40*, 2563–2570.
- (18) (a) Jeffrey, P. D.; Russo, A. A.; Polyak, K.; Gibbs, E.; Hurwitz, J.; Massague, J.; Pavletich, N. P. Mechanism of CDK activation revealed by the structure of cyclinA-CDK2 complex. *Nature* **1995**, *376*, 313–320. (b) Pavletich, N. P. Mechanisms of Cyclin-dependent Kinase Regulation: Structures of Cdks, their Cyclin Activators, and Cip and INK4 Inhibitors. *J. Mol. Biol.* **1999**, *287*, 821–828.
- (19) Shewchuk, L.; Hassell, A.; Wisely, B.; Rocque, W.; Holmes, W.; Veal, J.; Kuyper, L. F. Binding Mode of the 4-Anilinoquinazoline Class of Protein Kinase Inhibitor: X-ray Crystallographic Studies of 4-Anilinoquinazolines Bound to Cyclin-Dependent Kinase 2 and p38 Kinase. *J. Med. Chem.* **2000**, *43*, 133–138.
- (20) Lee, F. Y. F.; Borzilleri, R.; Fairchild, C. R.; Kim, S. H.; Long, B. H.; Raventos-Suarez, C.; Vite, G. D.; Rose, W. C.; Kramer, R. A. BMS-247550: A novel epothilone analogue with a mode of action similar to paclitaxel but possessing superior antitumor efficacy. *Clin. Cancer Res.* **2001**, *7*, 1429–1437.
- (21) Bol, D. K.; Dell, J.; Ho, C. J.; Swerdel, M.; Rowley, B.; Mulheron, J. G.; Webster, K. Dysregulation of cdk2 and cyclin E in the mouse skin: impacts on cell proliferation and tumorigenesis. Poster no. 2974, AACR Conference, San Francisco, U.S.A., April 1–5, 2000.
- (22) Dess, D. B.; Martin, J. C. Readily Accessible 12-I-5 Oxidant for the Conversion of Primary and Secondary Alcohols to Aldehydes and Ketones. *J. Org. Chem.* **1983**, *48*, 4155–4156.
- (23) Long, B. H.; Wang, L.; Lorico, A.; Wang, R. R. C.; Brattain, M. G.; Casazza, A. M. Mechanisms of resistance to etoposide and teniposide in acquired resistant human colon and lung carcinoma cell lines. *Cancer Res.* **1991**, *51*, 5275–5284.
- (24) Giannakakou, P.; Sacket, D. L.; Kang, Y.-K.; Zhan, Z.; Buters, J. T. M.; Fojo, T.; Poruchynsky, M. S. Paclitaxel-resistant human ovarian cancer cells have mutant β -tubulins that exhibit impaired paclitaxel-driven polymerization. *J. Biol. Chem.* **1997**, *272*, 17118–17125.

JM0201520